

NRC Research and/or Technical Assistance Rept

Por

EGG-SEMI-5940

JULY 1982

QUICK LOCK REPORT FOR SEMISCALE MOD-2A FEEDWATER

LINE BREAK TESTS S-SF-1, S-SF-2 AND S-SF-3

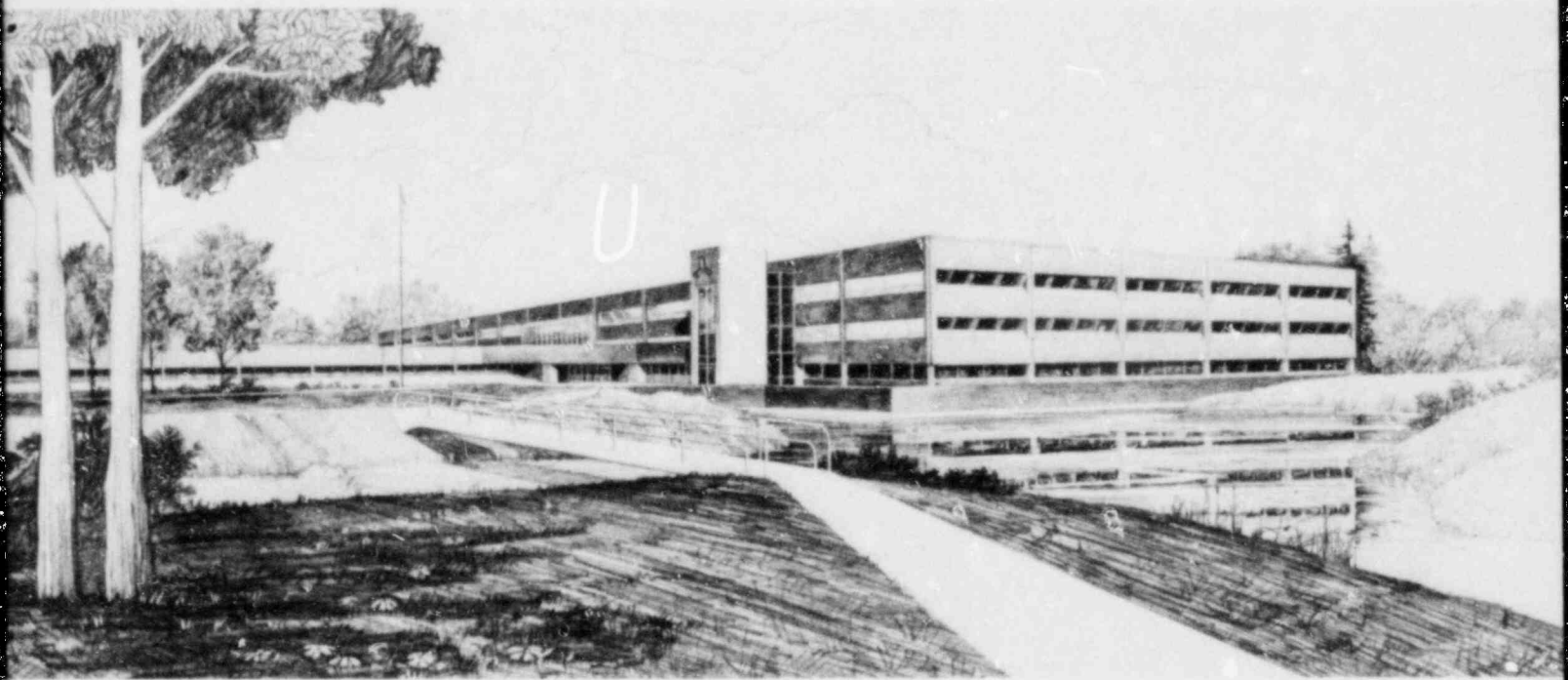
D. J. Shimeck

L. J. Martinez

G. R. Berglund

U.S. Department of Energy

Idaho Operations Office • Idaho National Engineering Laboratory



This is an informal report intended for use as a preliminary or working document

Prepared for the U.S. Nuclear
Regulatory Commission under DOE
Contract No. DE-AC07-761D01570
FIN No. A6038

8209280504 820731

PDR RES

8209280504

PDR





FORM EG&G-398
(Rev. 11-79)

INTERIM REPORT

Accession No. _____

Report No. EGG-SEM1-5940

Contract Program or Project Title:

Semiscale

Subject of this Document:

Quick Look Report for Semiscale Mod-2A Feedwater Line Break
Tests S-SF-1, S-SF-2 and S-SF-3

Type of Document:

Quick Look Report

Author(s):

D. J. Shimeck
L. J. Martinez
G. R. Berglund

Date of Document:

July 1982

Responsible NRC Individual and NRC Office or Division:

R. R. Landry, Reactor Safety Research

This document was prepared primarily for preliminary or internal use. It has not received full review and approval. Since there may be substantive changes, this document should not be considered final.

EG&G Idaho, Inc.
Idaho Falls, Idaho 83415

Prepared for the
U.S. Nuclear Regulatory Commission
Washington, D.C.
Under DOE Contract No. **DE-AC07-76ID01570**
NRC FIN No. A6038

INTERIM REPORT

QUICK LOOK REPORT FOR
SEMISCALE MOD-2A FEEDWATER LINE BREAK
TESTS S-SF-1, S-SF-2 AND S-SF-3

by

D. J. Shimeck

L. J. Martinez

G. R. Berglund

July 1982

Approval: _____

David Shimeck for GWS
G. W. Johnsen, Manager
WRRTF Experiment Planning
and Analysis Branch

Approval: _____

Paul North
P. North, Manager
Water Reactor Research
Test Facilities Division

CONTENTS

ABSTRACT	viii
SUMMARY	ix
1. INTRODUCTION	1
2. SYSTEM CONFIGURATION AND TEST CONDUCT	4
2.1 System Configuration	4
2.2 Test Procedures and Conditions	7
2.2.1 Preblowdown Activities	7
2.2.2 Component Controls	13
2.2.3 Changes and Discrepancies	17
3. TEST RESULTS	19
3.1 General Response	19
3.2 Secondary Response	22
3.3 Primary Response	31
3.4 Primary-to-Secondary Heat Transfer	50
3.5 Recovery Operations	56
4. CONCLUSIONS	62
5. REFERENCES	63

FIGURES

1.	Depiction of configuration assumed for feedwater line break scenario	3
2.	Semiscale Mod-2A as configured for feedwater line break experiments	5
3.	Cross-section of the Semiscale Mod-2A steam generators	6
4.	Broken loop steam generator; detail of steam dome	8
5.	Broken loop steam generator; detail of tube sheet and lower secondary volume	9
6.	Feedwater line break nozzles	10
7.	Core power for tests S-SF-1, S-SF-2 and S-SF-3	14
8.	Auxiliary feedwater flow rates to the broken and intact steam generators during Tests S-SF-1, S-SF-2 and S-SF-3	15
9.	HPIS flowrates for Tests S-SF-1, S-SF-2 and S-SF-3	16
10.	Comparison of primary and secondary pressures for Tests S-SF-1, S-SF-2 and S-SF-3	20
11.	Core power and system pressure vs. time for Tests S-SF-1, S-SF-2 and S-SF-3	21
12.	Broken loop steam generator mass inventory for Tests S-SF-1, S-SF-2, and S-SF-3	25
13.	Flow rate from feedwater line break for Tests S-SF-1, S-SF-2 and S-SF-3	26
14.	Fluid densities upstream of break for Tests S-SF-1, S-SF-2 and S-SF-3	27
15.	Collapsed liquid levels in the broken loop steam generator for Test S-SF-1	28
16.	Collapsed liquid levels in the broken loop steam generator for Test S-SF-2	29
17.	Collapsed liquid levels in the broken loop steam generator for Test S-SF-3	30
18.	Collapsed liquid levels in the intact loop steam generator for Test S-SF-1	32
19.	Collapsed liquid levels in the intact loop steam generator for Test S-SF-2	33

FIGURES (Continued)

20.	Collapsed liquid levels in the intact loop steam generator for Test S-SF-3	34
21.	Comparison of primary pressures for Tests S-SF-1, S-SF-2 and S-SF-3	35
22.	Primary pressurization in response to secondary heat sink degradation, Test S-SF-1	36
23.	Primary pressurization in response to secondary heat sink degradation, Test S-SF-2	37
24.	Primary pressurization in response to secondary heat sink degradation, Test S-SF-3	38
25.	Collapsed liquid levels in the pressurizer as calculated with saturated liquid density. (S-SF-2 data has been adjusted to compensate for instrument offset.)	40
26.	Pressurizer surge line differential pressure during secondary blowdown for Tests S-SF-1, S-SF-2 and S-SF-3	41
27.	Static pressure downstream of the broken loop pump	42
28.	Upper head and upper plenum temperatures for Test S-SF-1	44
29.	Upper head and upper plenum temperatures for Test S-SF-2	45
30.	Upper head and upper plenum temperatures for Test S-SF-3	46
31.	Upper head and upper plenum collapsed liquid levels from hot leg centerline, Test S-SF-1	47
32.	Upper head and upper plenum collapsed liquid levels from hot leg centerline, Test S-SF-2	48
33.	Upper head and upper plenum collapsed liquid levels from hot leg centerline, Test S-SF-3	49
34.	Change in heat transfer rate to broken loop secondary as a function of secondary inventory	51
35.	Comparison of primary fluid, tube metal, and secondary fluid temperatures at 452 cm above tube sheet in broken loop steam generator	52
36.	Local heat transfer rates in the broken loop steam generator during Tests S-SF-1, S-SF-2 and S-SF-3. Scram is indicated by arrow	53

FIGURES (Continued)

37.	Local heat transfer rates in the intact loop steam generator during Tests S-SF-1, S-SF-2 and S-SF-3	55
38.	Augmented core power from Test S-SF-3	57
39.	System pressure from Test S-SF-3	58
40.	Core and downcomer collapsed liquid levels from Test S-SF-3	60
41.	High and mid-core temperatures from Test S-SF-3	61

TABLES

1.	Initial conditions and ECC parameters for Tests S-SF-1, 2, 3	11
2.	Sequence of events for Semiscale feedwater line break experiments	23

ABSTRACT

Results are presented from a preliminary analysis of Semiscale Mod-2A Tests S-SF-1, 2, and 3. These experiments simulated various size breaks in the secondary side feedwater lines to a steam generator in a pressurized water reactor system. The experiments were initiated from nominal full power conditions. The primary objective of the experiments was to evaluate the primary-to-secondary heat transfer response resulting from a blowdown of the secondary side.

SUMMARY

This report presents the results of a preliminary analysis of data from Semiscale Mod-2A tests S-SF-1, 2, and 3. These experiments simulated breaks of various sizes in the secondary side feedwater line to the steam generators of a pressurized water reactor (PWR) system. The feedwater line break was postulated to occur in a line which is connected near the bottom of the steam generator. Such feedwater line breaks result in a pressurization of the primary due to the loss of secondary heat sink. The scenario simulated in the experiments disallowed any safety trips that may occur prior to a high pressurizer pressure signal. Auxiliary feedwater flow was delayed until the rapid transient portion of the experiments was over.

The primary objective of experiments was to evaluate the primary-to-secondary heat transfer behavior that accompanies a secondary blowdown. The series sought to provide a data base that is useful for evaluating the capabilities of water reactor safety computer codes to predict integral system response to secondary side transients. Specific quantitative behavior of the primary system was considered to be of secondary importance in analyzing the experiments.

The transients were initiated from full power conditions by opening a blowdown valve on the broken loop steam generator. Feedwater flow was terminated to both generators at time zero. The steam control valves were left in their initial position until a high primary pressure trip signal was received. Initially the primary depressurized slightly due to termination of pressurizer heating and a slight decrease in the secondary pressures. Eventually the heat transfer to the broken loop degraded very suddenly and the primary pressure rose rapidly to the trip point of 12.86 MPa. Trip points were reached in 40, 75, and 88 seconds, respectively, in the largest, middle and smallest breaks. However, the actual period of the primary pressure excursions was only about 15 to 20 s.

When the high pressure trip was reached the core was SCRAMed immediately. The primary pressure experienced a small overshoot after the

trip point and then rapidly decreased. An extended, slow depressurization then followed, governed by the injection of cold auxiliary feedwater to the intact loop secondary, heat losses to the environment, and HPIS cold water injection. The resulting primary fluid shrinkage caused some voiding of the upper regions of the vessel, but the system remained stable and well cooled in a natural circulation mode driven by the intact loop heat sink.

Analysis of the primary-to-secondary heat transfer behavior highlighted some interesting results. The degradation of heat transfer to the broken loop was found to occur within a few seconds throughout the entire length of the generator. It also occurred while there was substantial coolant inventory in the secondary side. The inventory at which degradation occurred was determined to be a function of break size, varying from a nominal 30% inventory for the smallest break size examined, up to approximately 90% for the largest. In terms of inventory, the heat transfer coefficient degraded fully over only about a 10% change in inventory. This behavior, along with limited secondary side temperature information, suggests that the degradation in heat transfer is due to a large change in secondary side hydraulic conditions on the surface of the tubes rather than being associated predominantly with a loss of secondary inventory.

Analysis of the data indicates that the predominant distortions stemming from discrepancies in system conditions and configuration in relation to a PWR were in regard to timing of transient events. The phenomenological information gathered is felt to be useful and valid.

QUICK LOOK REPORT FOR
SEMISCALE FEEDWATER LINE BREAK TESTS S-SF-1, 2, AND 3

1. INTRODUCTION

Testing performed in the Semiscale Mod-2A system is part of the water reactor safety research effort directed toward assessing and improving the analytical capability of computer codes which are used to predict the behavior of pressurized water reactors (PWRs) during postulated accident scenarios. For this purpose, the Mod-2A system was designed as a small-scale model of the primary system of a four-loop PWR nuclear generating plant. The system incorporates the major components of a PWR including steam generators, vessel, pumps, pressurizer, and loop piping. One loop (intact loop) is scaled to simulate three coolant loops in a PWR, while the other (broken loop) simulates a single loop. Geometric similarity has been maintained between a PWR and Mod-2A, most notably in the design of a 25 rod, full-length (3.66 m), electrically heated core, full-length upper head and upper plenum, component layout, and relative elevations of various components. The scaling philosophy followed in the design of the Mod-2A system (modified volume scaling) preserves most of the important first-order effects thought important in simulating transients which may occur in a PWR.

This report presents a preliminary analysis of data from Semiscale Tests S-SF-1, 2, and 3. These tests were experiments simulating secondary side feedwater line breaks of various sizes. The primary objective of the SF test series¹ is to evaluate the primary-to-secondary heat transfer behavior that accompanies a blowdown of the steam generator secondaries. Data from the series will provide a reference data base for evaluating the capabilities of water reactor safety codes to predict integral system response to secondary side transients. Additionally, the tests will be used to provide scoping information for any further secondary transient testing deemed necessary. Two further experiments in the SF series (Tests S-SF-4 and 5) will simulate main steam line breaks.

Figure 1 presents a simple depiction of the scenario assumed for the feedwater line break experiments. The transient is initiated by a pipe break downstream of the check valve on one steam generator. Feedwater flow is terminated to both generators due to the pressure differential across the check valve on the intact line. Communication exists between the two generators through the steam lines until the main steam isolation valves are closed. This was simulated in the Semiscale system by leaving the two independent steam control valves in their initial position. All safety trips (e.g., low secondary level) are considered to be overridden until a high primary pressure trip occurs. Auxiliary feedwater is not injected until after the pressurization portion of the transient is over.

A preliminary experiment analysis is presented in the following sections. Section 2 describes the system hardware, test conduct, and initial conditions. Section 3 presents the results from the test analysis, and Section 4 presents conclusions drawn from the preliminary evaluation.

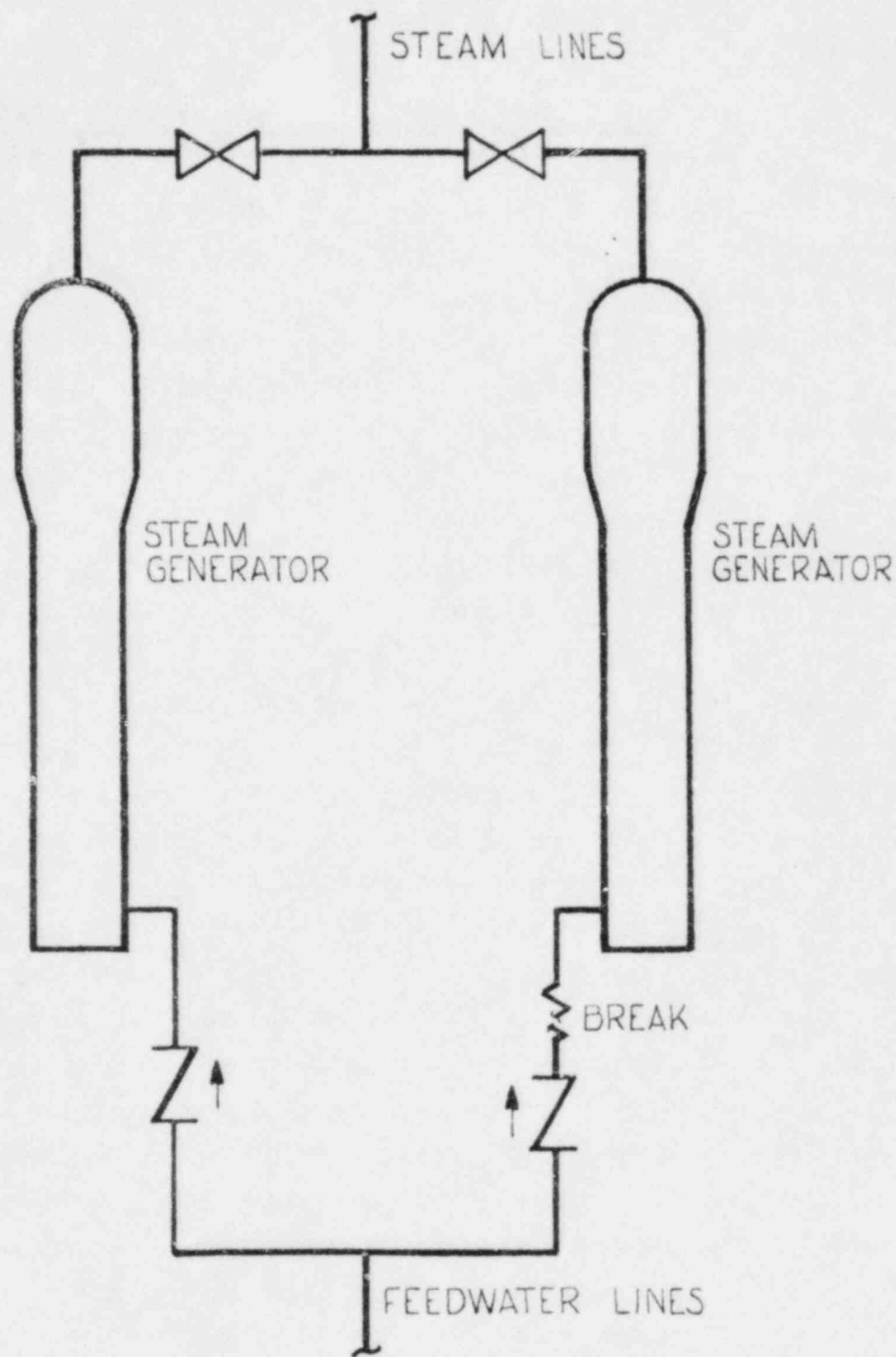


Figure 1. Depiction of configuration assumed for feedwater line break scenario.

2. SYSTEM CONFIGURATION AND TEST CONDUCT

2.1 System Configuration

For Semiscale Mod-2A Tests S-SF-1, 2, and 3 the Mod-2A system was configured as shown in Figure 2. The major components of the system were the vessel with electrically heated core and external downcomer, intact and broken loop steam generators, intact and broken loop recirculation pumps, and loop piping. The vessel core consists of a 5 x 5 array of internally heated electric rods, 23 of which were powered. The rods are geometrically similar to nuclear rods with a heated length of 3.66 m and an outside diameter of 2.072 cm. All 23 heated rods were powered equally. The primary system also incorporated the use of external heaters on loop piping and on the pressure vessel to mitigate the effects of heat loss to the environment. A more detailed description of the Mod-2A system may be found in References 1 and 2. The following paragraphs highlight important features of the steam generators that are of interest for these experiments.

Both the intact loop and broken loop steam generators are of a tube and shell design. Primary fluid flows through vertical, inverted, U-shaped tubes and secondary coolant passes through the shell side. The intact loop steam generator has two short, two medium, and two long tubes representative of the range of bend elevations in a PWR steam generator. The broken loop steam generator has only two tubes, a long tube and a short tube both of which are identical to the intact loop generator long and short tubes. The same tube stock (2.22 cm O.D. x 0.124 cm wall thickness) and tube spacing (3.175 cm triangular pitch) used for PWR U-tubes is used in the Mod-2A design. Since the heat transfer area was based on the ratio of PWR to Semiscale core power, the number of tubes was therefore determined by the specified tube diameter and lengths. Filler pieces are installed in the shell side to provide a more properly scaled secondary fluid volume. A cross-sectional plan view of the intact and broken loop steam generator U-tubes and filler pieces is shown in Figure 3.

Elevations of the steam generator nozzles, plenums, and tubes are similar to those of a PWR. The steam dome is shorter than the steam dome

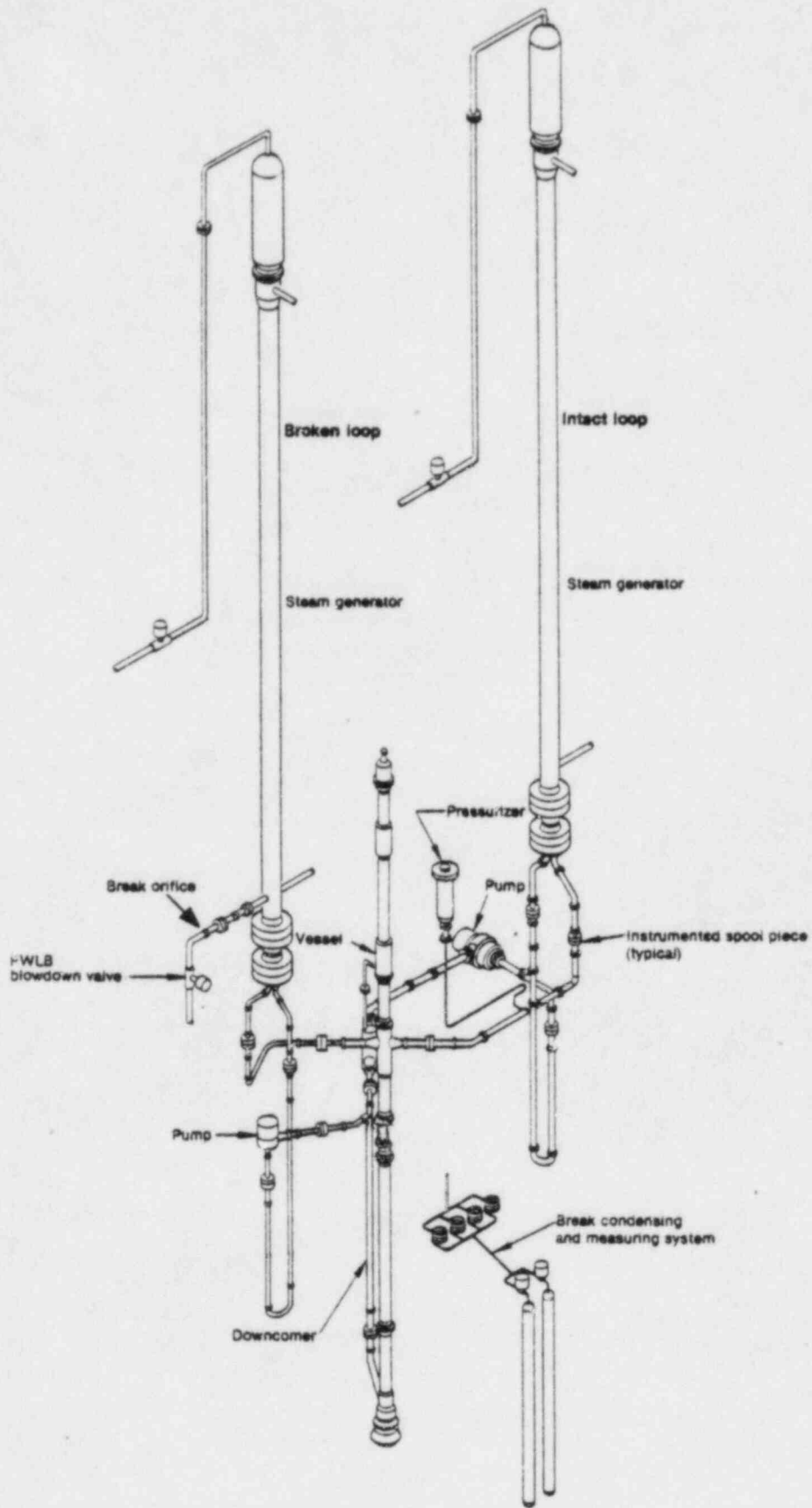


Figure 2. Semiscale Mod-2A as configured for feedwater line break experiments.

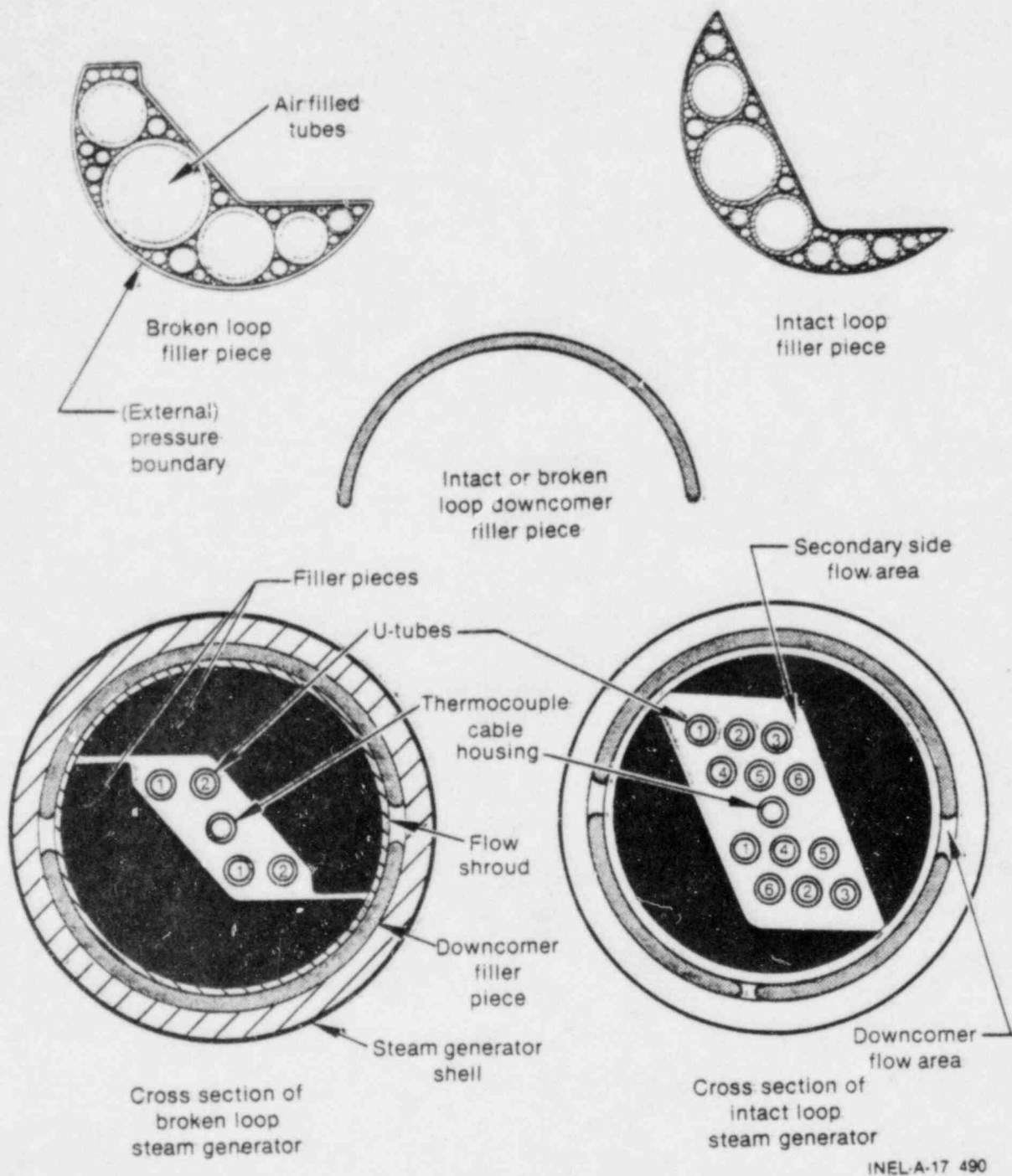


Figure 3. Cross-section of the Semiscale Mod-2A steam generators.

in a PWR and the steam drying equipment is of a simpler and less efficient design. Figure 4 is a detail of the steam dome region showing the centrifugal vane separator and the annulus configuration.

As seen in Figure 5 the lower portion (approximately one-half meter) of the downcomer is of an annular geometry. The majority of the downcomer length consists of two (broken loop) or three (intact loop) flow channels that connect the steam dome and lower downcomer annular regions (see also Figure 3). This configuration is used to reduce the fluid volume of the downcomer region. Feedwater enters the steam generators at a point 36 cm above the tube sheet. The feedwater mixes with recirculated water from the downcomer and enters the riser section where the tubes are located through four slots in the flow divider. For these tests auxiliary feedwater was injected into a spray ring at the lower end of the steam dome annulus.

For the feedwater line break tests the broken loop steam generator was modified to incorporate a break measurement spool and nozzle assembly. Figures 2 and 5 illustrate respectively, the relative location of the break assembly, and the location of the break port in relation to the steam generator internals. Three different break sizes were simulated. The sizes and details of the break nozzles are shown in Figure 6. The break assembly consisted of a valve downstream of the break nozzle and a drag screen-densitometer measurement upstream. Additionally, for the smallest break size (Test S-SF-3) the break effluent was condensed, collected and measured in a catch tank system.

2.2 Test Procedures and Conditions

2.2.1 Preblowdown Activities

Prior to initiation of the transients the Semiscale system was stabilized at the initial conditions listed in Table 1. Priority was given to establishing the correct core power, primary pressure, cold leg temperature, and core differential temperature. The loop flow rates and secondary side pressures were adjusted as necessary. The indicated liquid levels on the secondaries were kept within a selected band by throttling

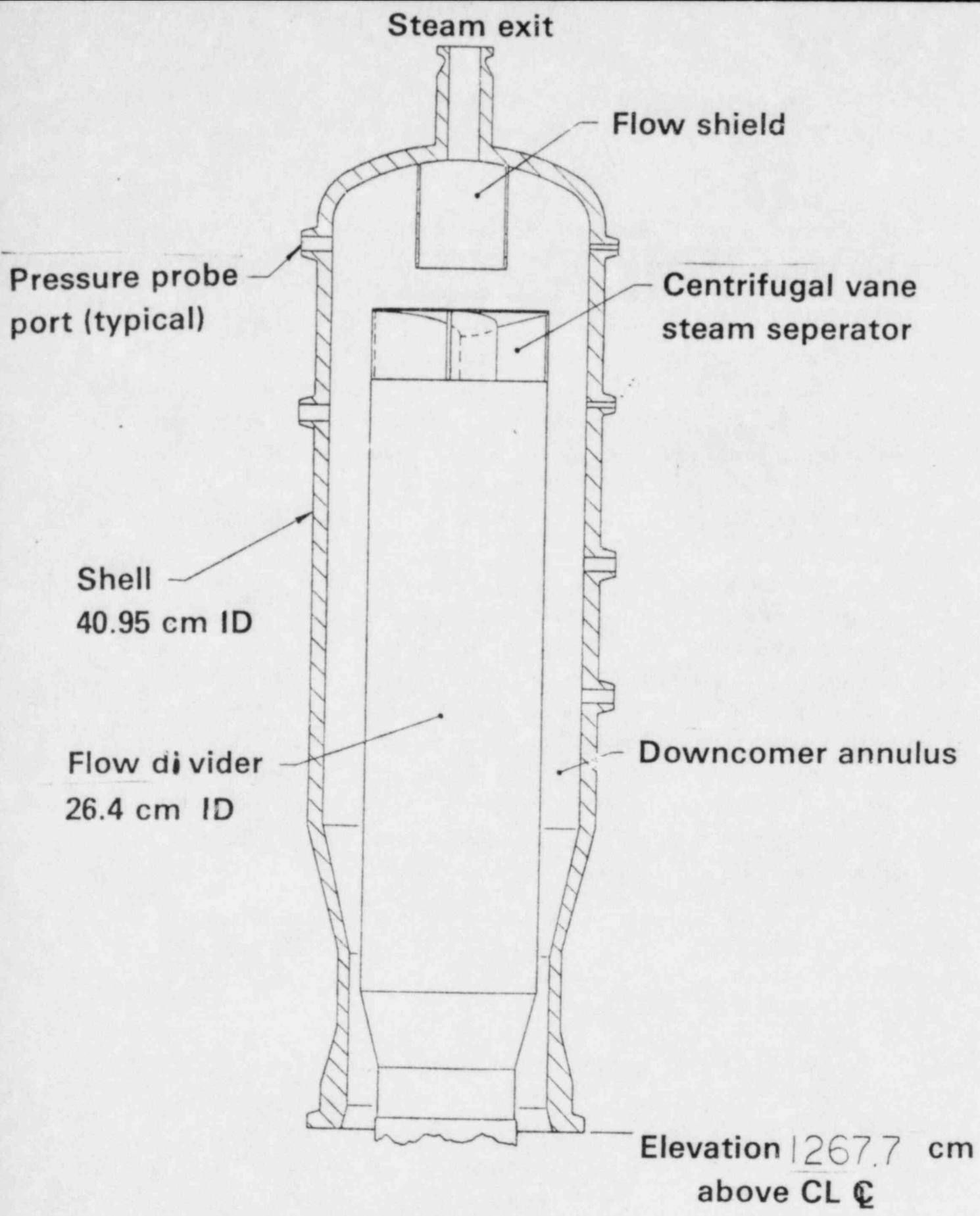


Figure 4. Broken loop steam generator; detail of steam dome.

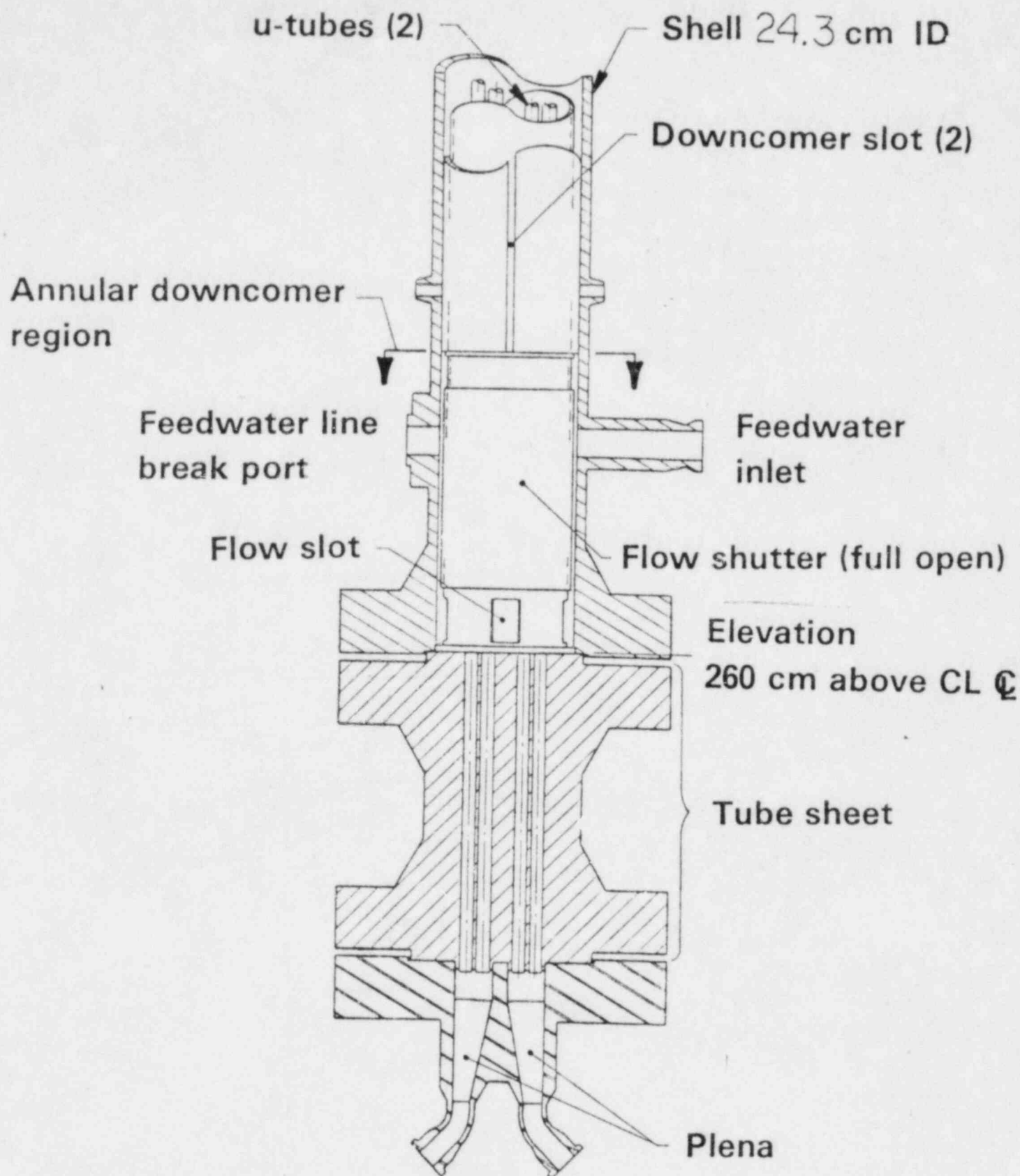
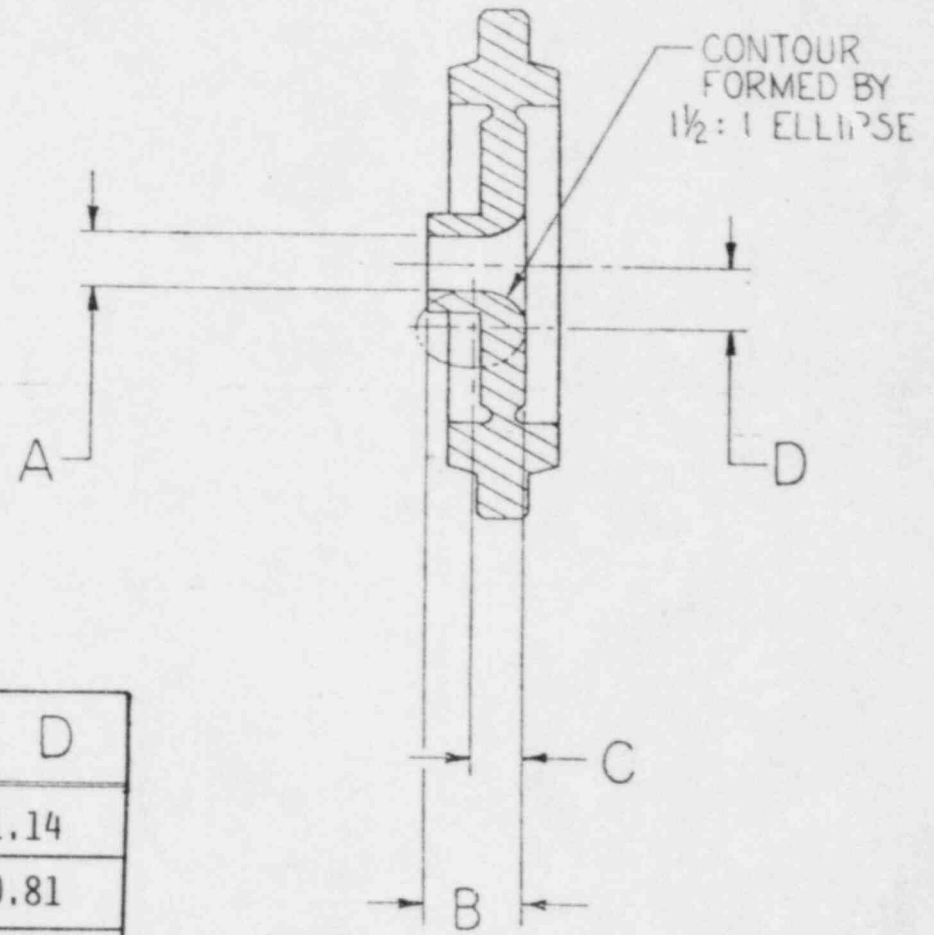
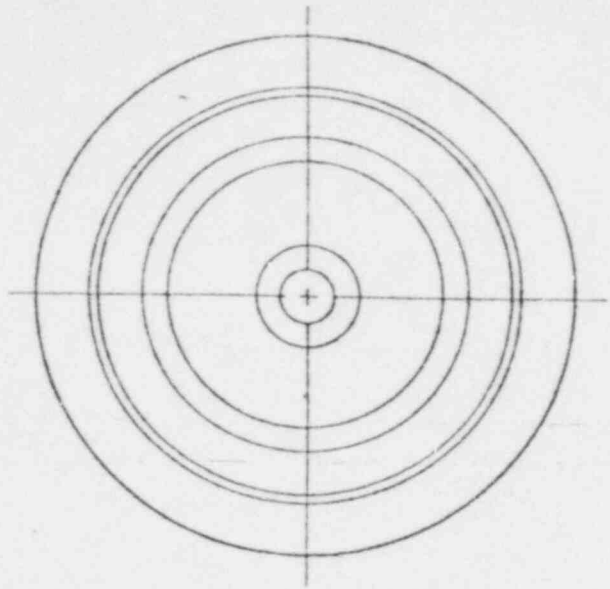


Figure 5. Broken loop steam generator; detail of tube sheet and lower secondary volume.



10

TEST	A	B	C	D
S-SF-1	0.978	1.27	0.978	1.14
S-SF-2	0.691	1.27	0.691	0.81
S-SF-3	0.368	0.63	0.368	0.43

NOTE: DIMENSIONS IN CM.

Figure 6. Feedwater line break nozzles.

TABLE 1. INITIAL CONDITIONS AND ECC PARAMETERS FOR TESTS S-SF-1, 2, 3

Parameter	Value		
	S-SF-1	S-SF-2	S-SF-3
<u>Initial Conditions</u>			
Pressurizer pressure	15.15 MPa	15.53 MPa	15.15 MPa
Core temperature differential	35 K	35 K	35 K
Cold leg fluid temperature			
Intact loop	561 K	562 K	563 K
Broken loop	560 K	568 K	561 K
Total core power	2 MW	2 MW	2 MW
Radial power peaking	Flat	Flat	Flat
Pressurizer liquid mass	9.42 kg	6.12 kg ^a	12.4 kg
S. G. secondary pressure			
Intact loop	6.24 MPa	6.15 MPa	6.31 MPa
Broken loop	6.30 MPa	7.36 MPa	6.45 MPa
S. G. feedwater temperature			
Intact loop	528 K	529 K	528 K
Broken loop	522 K	525 K	525 K
S. G. secondary water mass			
Intact loop	80 kg	99 kg	114 kg
Broken loop	152 kg	172 kg	126 kg
S. G. feedwater flow rate (-20 s < t < 0.5)			
Intact loop	1.0 kg/s	1.2 kg/s	1.0 kg/s
Broken loop	0.12 kg/s	0.084 kg/s	0.25 kg/s
<u>Configuration</u>			
Break size	.978 cm ID	.691 cm ID	.368 cm ID
Break type	Noncommunicative	Noncommunicative	Noncommunicative
Break location	Feedwater line	Feedwater line	Feedwater line
Pressurizer location	Intact loop	Intact loop	Intact loop
Pressurizer line resistance	$3.36 \times 10^9 \text{ m}^{-4}$	$3.36 \times 10^9 \text{ m}^{-4}$	$3.36 \times 10^9 \text{ m}^{-4}$
Pressurizer relief valve			
Setpoint	16.31 MPa	16.31 MPa	16.31 MPa
Orifice size	0.29 cm	0.29 cm	0.29 cm
<u>ECC Injection</u>			
I.L. HPIS			
Actuation pressure	10.7 MPa	10.23 MPa	10.85 MPa
Injection rate	0.035 L/s	0.037 L/s	0.032 L/s
Temperature	296 K	298 K	300 K

TABLE 1. (Continued)

Parameter	Range		
	S-5-1	S-5-2	S-5-3
<u>Transient Conditions</u>			
SCRAM (power decay)			
Pressure setpoint ^{b,c}	15.7 MPa	15.7 MPa	15.5 MPa
Time delay	0.0 s	0.0 s	0.0 s
Steam generator controls			
Relief valve setpoint			
Intact loop ^a	8.03 MPa	8.03 MPa	8.03 MPa
Broken loop ^a	8.03 MPa	8.03 MPa	8.03 MPa
Auxiliary feedwater flow			
Initiation	100 s	100 s	150 s
Flowrate			
Intact loop	.014 ± .009 1/s	.042 ± .015 1/s	.04 ± .008 1/s
Broken loop	.014 1/s	.014 1/s	.014 1/s
Leakage			
Initial rate ^a	.005 kg/s	.008 kg/s	.005 1/s

- a. These values are either taken from or calculated with process measurements.
- b. Pressurizer pressure.
- c. SCRAM was initiated at 15.86 MPa as determined by process instrumentation.

the feedwater as necessary.^a Once conditions had been established within allowable tolerances the transients were initiated by opening the blowdown valve on the feedwater line break assembly. Just prior to this the feedwater control valves from the feedwater supply tank were closed and the pressurizer heaters were turned off.

2.2.2 Component Controls

Core power, primary recirculation pump speeds, and steam line control valve positions were maintained constant until a high pressurizer pressure trip signal was received. At that time the core power was ramped down as shown in Figure 7. The primary coolant pumps were also coasted down per curves in Reference 1. Secondary side auxiliary feedwater injection was manually initiated at a preselected time; 100 s for Tests S-SF-1 and 2, and 150 s for Test S-SF-3 which was a slower transient. The injection flow rates vs time are shown in Figure 8. Auxiliary flow to the broken loop was terminated at about 300 s to simulate operator action in response to identifying the affected generator. The flow control on the intact loop auxiliary feedwater pump was found to be pressure sensitive, in addition to having some drift, and therefore resulted in the varying rate seen in Figure 8.

HPIS injection was initiated on low primary pressure. The injection rates are shown in Figure 9. The rate was determined by a flow versus primary pressure curve in Reference 1. After substantial upper vessel voiding was observed the HPIS flow rate was increased to expedite system recovery in Tests S-SF-1 and 2. A primary feed and bleed recovery scoping test was attempted in Test S-SF-3 as described more completely in Section 3.5.

a. Conditions are generally insensitive to secondary inventory.

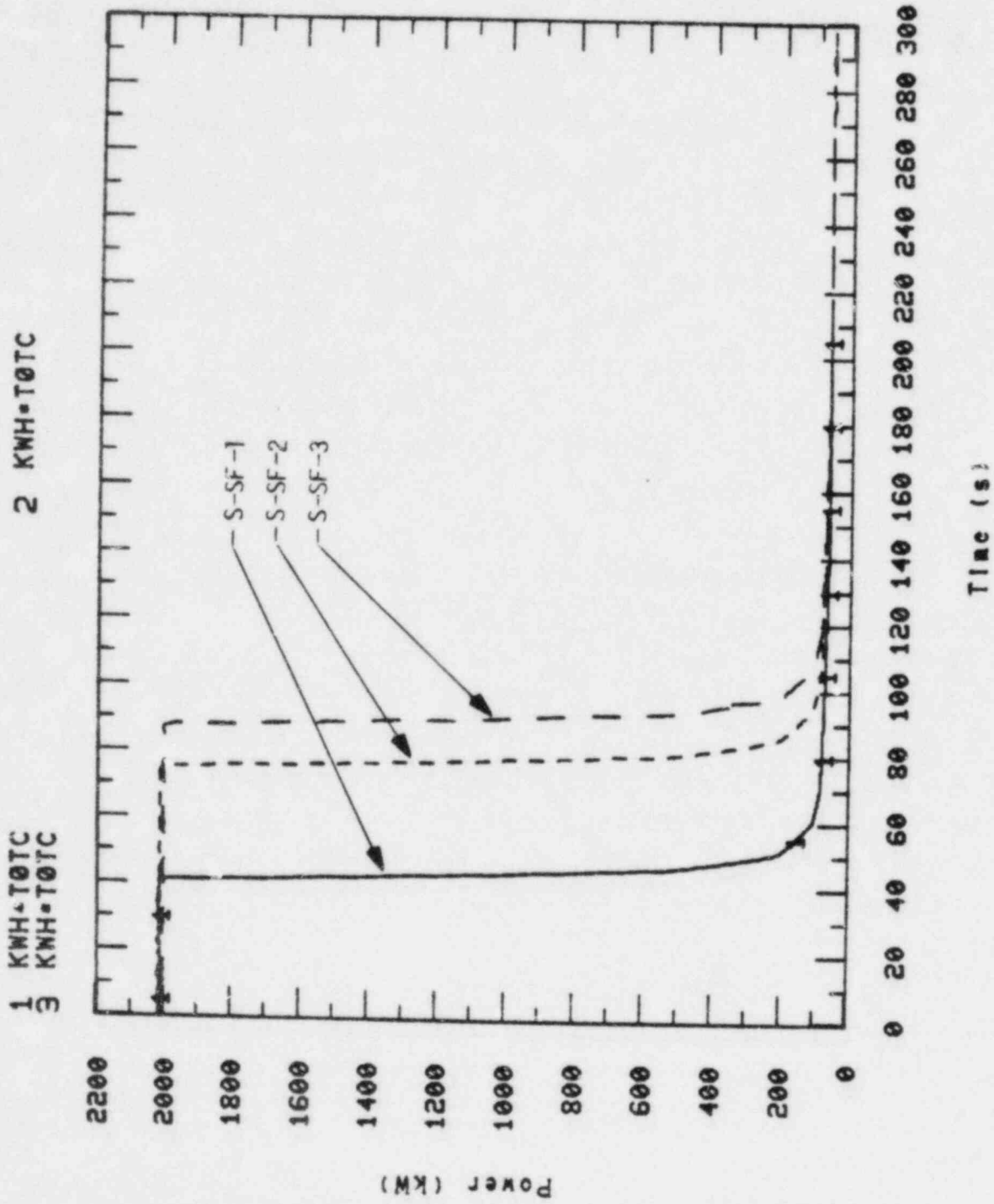


Figure 7. Core power for tests S-SF-1, S-SF-2 and S-SF-3.

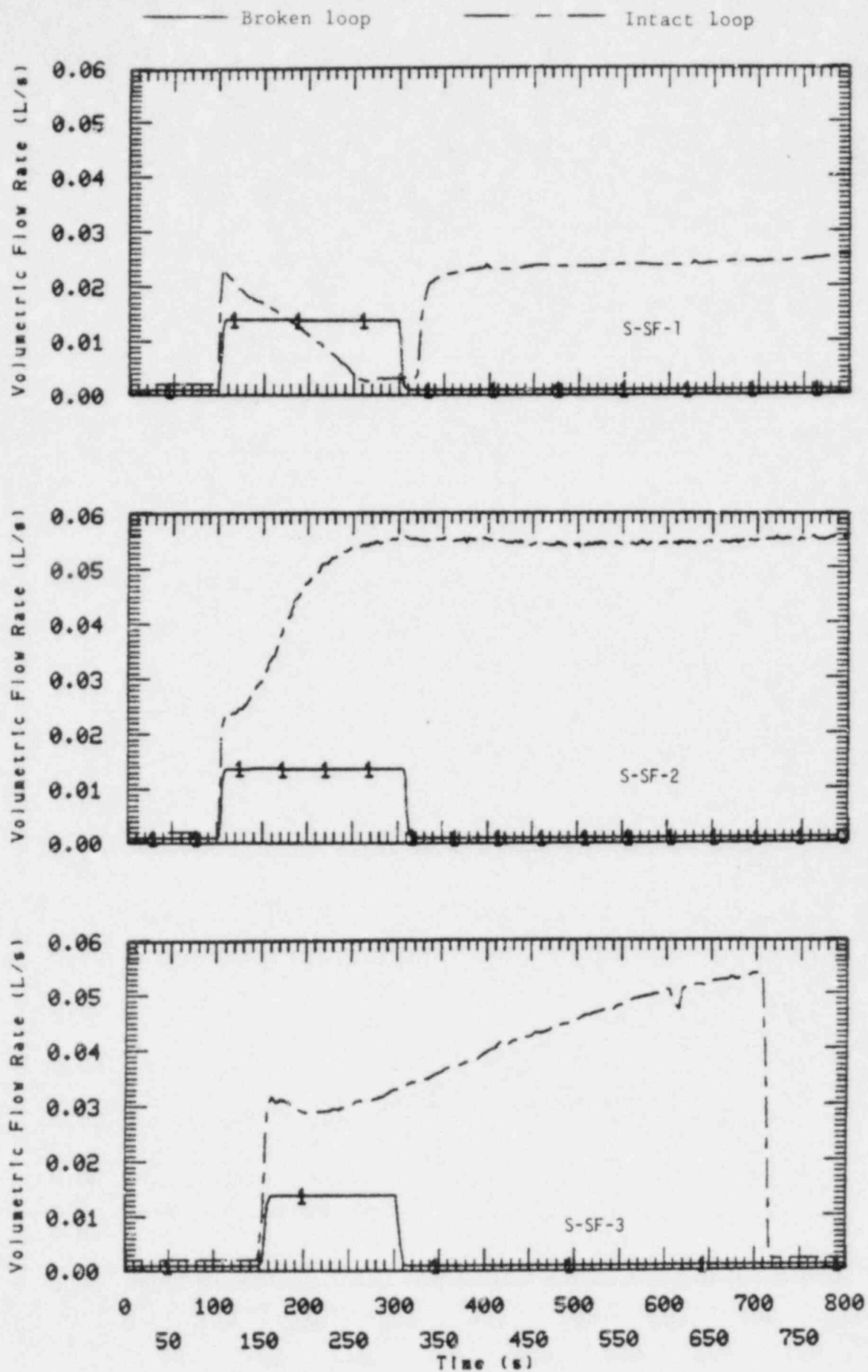


Figure 8. Auxiliary feedwater flow rates to the broken and intact steam generators during Tests S-SF-1, S-SF-2, and S-SF-3.

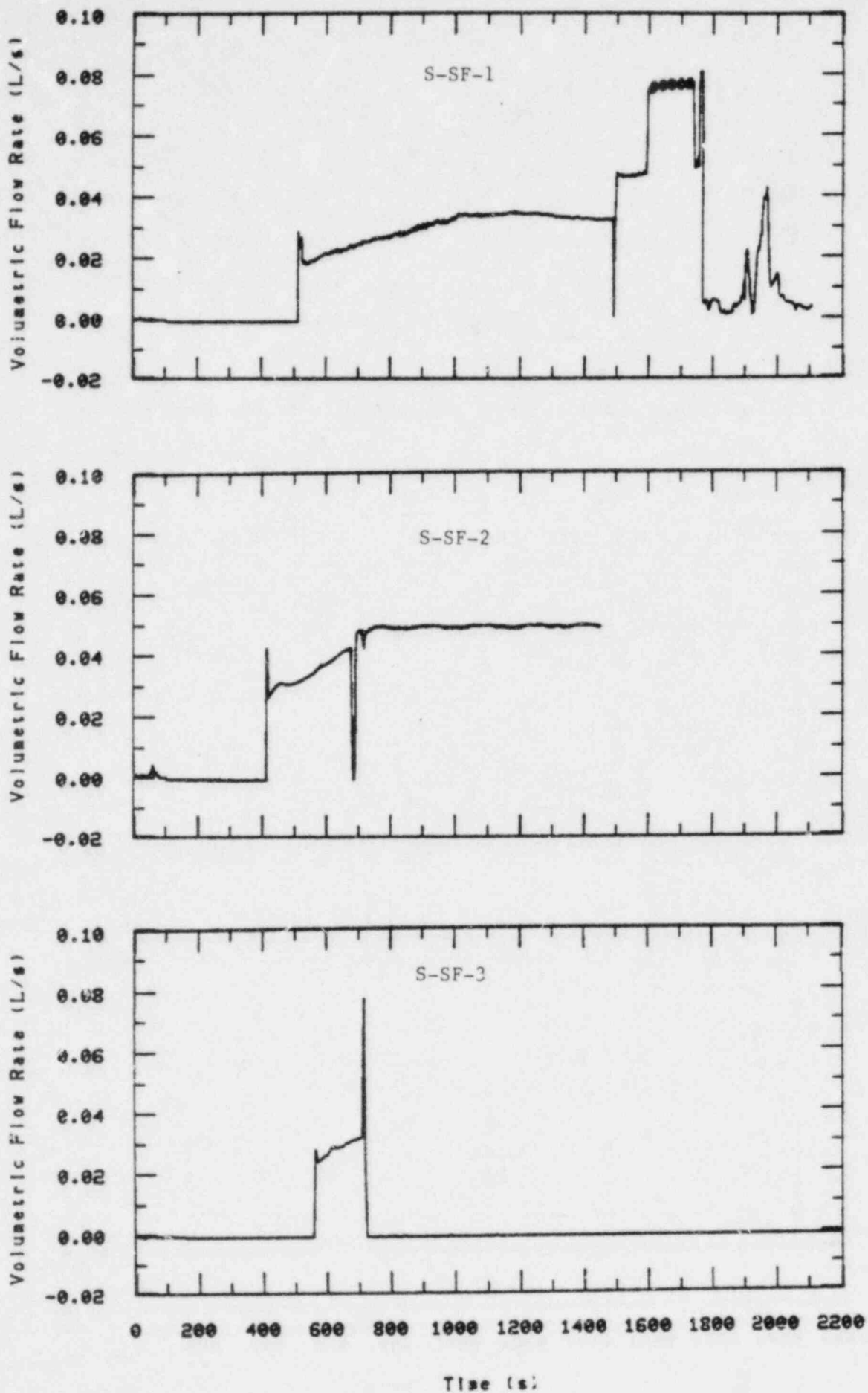


Figure 9. HPIS flowrates for Tests S-SF-1, S-SF-2, and S-SF-3.

2.2.3 Changes and Discrepancies

Changes are occasionally incorporated into test plans as a series progresses to improve the quality of the results, and some discrepancies occur during the conduct of testing. The following points are noteworthy with regard to Tests S-SF-1, 2, and 3.

The secondary volumes of the steam generators as reported in References 1 and 2 were found to be in error. The correct volumes of the secondaries up to the top of the tubes (1000 cm above the tube sheet) are in actuality; broken loop: 125 L, intact loop: 200 L. These values represent differences of about 100% and 40% respectively from previously reported volumes. In conjunction with the operating characteristics of the steam generators this produced large discrepancies in secondary inventory both in relation to the originally specified conditions and in conditions from test to test. These discrepancies are shown in the Results section not to have prohibited the tests from meeting the primary objective of evaluating primary-to-secondary heat transfer behavior. Since the break sizing, in terms of percent break size, was based upon preserving the time to empty of the broken loop secondary, these break sizes are therefore effectively smaller than the values given in Reference 1. Using the scaling logic presented in Appendix A of Reference 1, which sought to preserve the time to empty of the broken loop steam generator based upon ratioing the reference plant and Semiscale Mod-2A secondary masses, the equivalent break sizes for a full-size plant would be; Test S-SF-1: 0.035 m^2 , Test S-SF-2: 0.015 m^2 , Test S-SF-3: 0.006 m^2 . The most prominent distortion caused by the inventory differences appears to be merely a change in the timing of transient events.

A second discrepancy involves the broken loop/intact loop heat load split at initial conditions. Due to errors in process measurements used to control the system the broken loop heat load for these tests was typically 20% of the total, versus the correctly distributed value of 25%. The predominant effect of this was to distort the primary pressurization response which was of secondary importance to the experimental objectives.

A change that was invoked for Tests S-SF-1 and 3 (conducted following Test S-SF-2) was a lowering of the initial primary pressure to 15.17 MPa from 15.5 MPa and, in all tests, a lowering of the high pressure trip point to 15.86 MPa from 16.2 MPa. This was done to allow better observation of the primary pressurization transient while affording more conservative system overpressurization protection. This change had negligible effect on the transient behavior.

3. TEST RESULTS

Preliminary results are presented in this section from the three feedwater line break tests, S-SF-1, S-SF-2, and S-SF-3. First, the general system response to the three different break sizes is briefly discussed, presenting a sequence of important events that occurred during the transients. A more detailed analysis of both the secondary and primary thermal-hydraulic behaviors is presented next, including a preliminary evaluation of heat transfer behavior in the steam generators. The recovery procedures used to maintain core cooling are then discussed, followed by the preliminary conclusions drawn from the experiments.

3.1 General Reponse

The secondary side blowdowns were initiated from full power steady-state conditions. As seen in Figure 10 a slight cooldown and depressurization of the primary occurred initially in each test, prior to the pressure excursion. This was caused by the termination of power to the pressurizer heaters at $t = 0$ (an operational procedure) in conjunction with a small depressurization of one or both secondaries. (Feedwater was terminated to both loops at $t = 0$). A very rapid degradation of primary-to-secondary heat transfer then occurred which led to rapid (25 to 48 kPa/s) pressurizations of the primary up to the SCRAM setpoint in a few seconds as seen in Figure 11. The core power was SCRAMed by a high pressurizer pressure signal of 15.86 MPa on the process control instrumentation. (Tests 1 and 3, which were conducted following Test 2, were initiated from a lower primary pressure in order to better examine the pressurization phenomena.)

Once the core had SCRAMed the pressure dropped rapidly to about 14 MPa and then slowly decreased for the remainder of the transient aided by the injection of secondary side auxiliary feedwater and heat losses to ambient. Concurrent with the SCRAM the steam lines were isolated. The intact loop steam generator quickly repressurized and then slowly cooled, and the broken loop pressure exponentially decreased to ambient pressure through the break. The broken loop auxiliary feedwater injection was

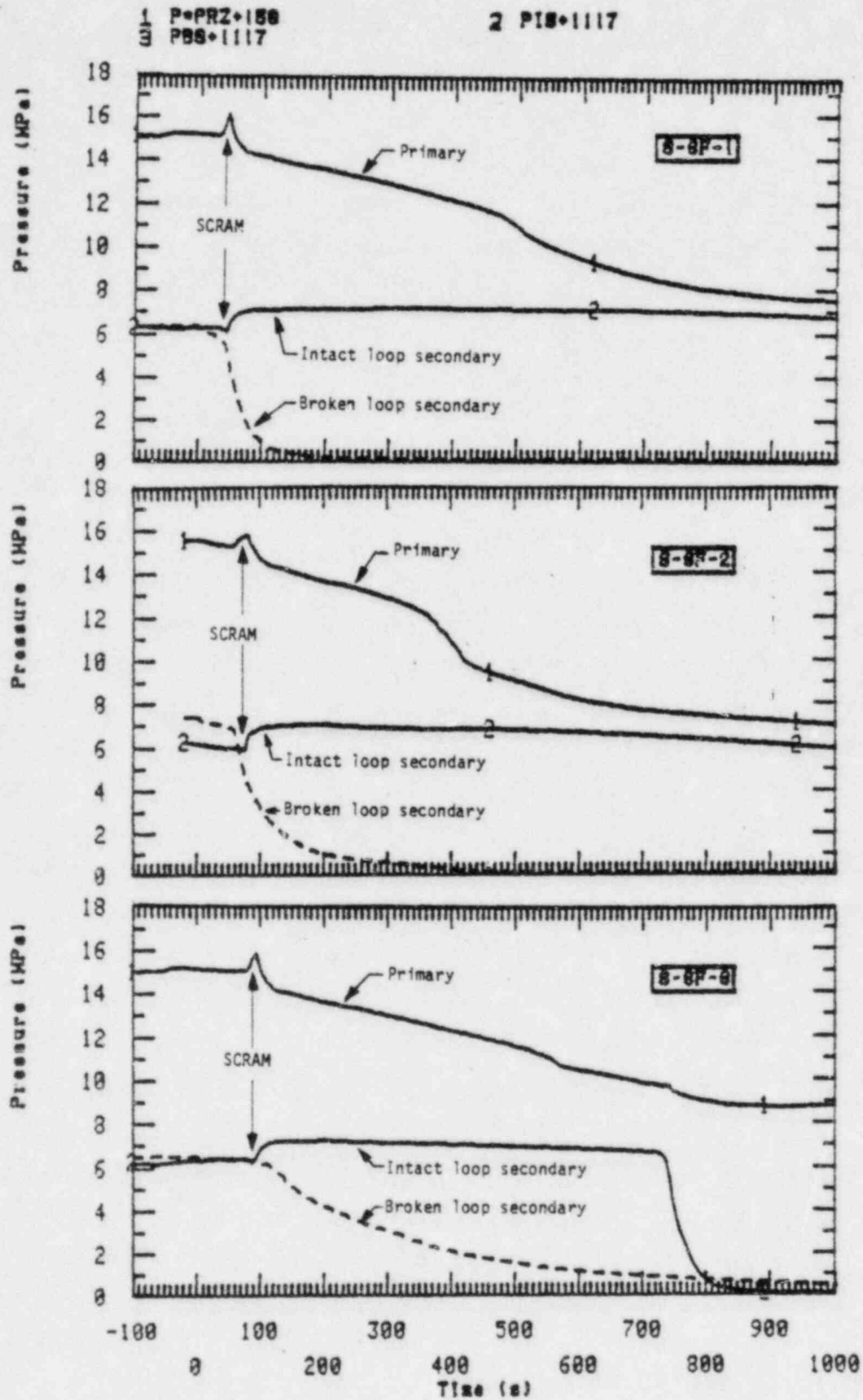


Figure 10. Comparison of primary and secondary pressures for Tests S-SF-1, S-SF-2, and S-SF-3.

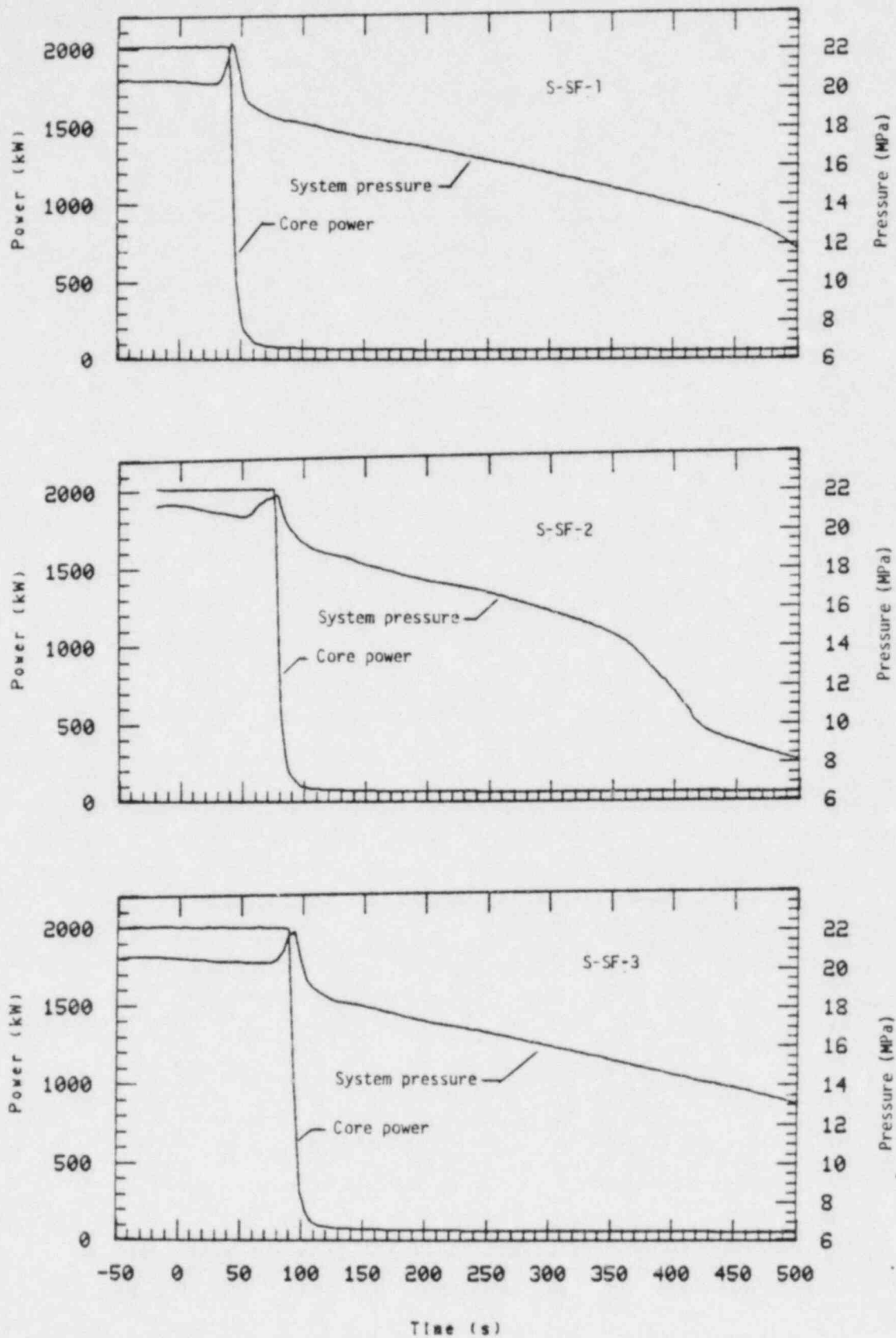


Figure 11. Core power and system pressure vs. time for Tests S-SF-1, S-SF-2, and S-SF-3.

terminated at about 300 s to simulate operator action. Intact loop auxiliary feedwater flow was left on and the tests were continued long enough to verify that the system was continuously cooling down. HPIS pumped ECC injection was activated automatically at 11.2 MPa.

The feedwater line break portion of Test S-SF-3 was terminated at 700 s in order to perform a recovery operation involving primary feed and bleed, which is discussed in Section 3.5. Table 2 summarizes the timing of important events that occurred during the experiments.

3.2 Secondary Response

At the initiation of the transients, feedwater flow was terminated to both loops. The steam control valves were left in their normal open position until a high primary pressure trip signal was received. Figure 10 compared the primary system pressures with both intact and broken loop secondary pressures. Neither loop underwent any significant depressurization at the initiation of the transients as generation of steam from boiling and flashing in the effected generator was sufficient to maintain pressure. When the trip signal was received the intact loop secondary was isolated and repressurized slightly. It then slowly depressurized for the remainder of the transients due to the injection of cold auxiliary feedwater and heat losses to the ambient (approximately 6 kW).

The broken loop steam generator pressure behavior was found to be a function of break size. Immediately following the break, as seen in Figure 10, for the largest break size a continuous depressurization begins. For the next smallest break there is a sharp drop at the time of the break, but then a much slower depressurization, while for the smallest break size the pressure remains relatively constant. The sources of heat involved in flashing the secondary fluid are; heat transferred from the primary to the secondary, bulk flashing from depressurization, and structural heat transfer. The latter two terms are interrelated since structural heat transfer is a function of the rate of change of $T_{sat}(P)$,

TABLE 2. SEQUENCE OF EVENTS FOR SEMISCALE FEEDWATER LINE BREAK EXPERIMENTS

Event	Time (s)		
	S-SF-1	S-SF-2	S-SF-3
Close feedwater valves	-2.0	-2.0	-2.0
Break	0	0	0
Primary pressure excursion begins	27	42	75
SCRAM	40	75	88
I.L. and B.L. steam valves begin closing	40	75	88
B.L. and I.L. pump coastdown initiated	40	75	88
Auxiliary feed initiated	100	105	150
B.L. auxiliary feed off	300	308	300
HPIS on	510	410	560
Vessel upper plenum voiding	620	440	860
Vessel upper head voiding	910	660	1130
Primary feed and bleed recovery initiated	N/A	N/A	3650
Termination	2100	1450	4500

and are therefore both are depressurization-governed terms. The larger the break size the smaller the significance of the primary-to-secondary heat transfer term, relative to the depressurization terms.

Eventually the broken loop pressure curves knee over and decrease rapidly as two-phase fluid reaches the break. Referring also to Figure 12 it is seen that this occurs even with significant water quantities remaining in the secondary. The inventory curves were generated taking into consideration the measured break flows, steam line flows, and auxiliary feedwater injection rates. Some interpretation was required in order to determine the initial inventories and those shown represent the best estimates. The flow out the steam line, as measured with a flow orifice, remained approximately constant from $t = 0$ to the time it was isolated. Figures 13 and 14 show, respectively, the break flow rate^a and the measured fluid density immediately upstream of the break. When the break is first opened a slug of cold water is expelled to clear the line. The density measurement is seen to indicate saturated liquid density within a few seconds. Depending upon break size the upstream condition remained nearly all liquid (S-SF-3, smallest break), showed a small amount of voiding (S-SF-2, middle break), or rapidly voided (S-SF-1, largest break) prior to emptying the generator.

The indicated liquid level behavior of the broken loop secondary side is shown in Figures 15 through 17. Shown in the figures are collapsed liquid levels obtained from differential pressure measurements over several different spans. No flow pressure drop corrections have been applied, and saturated liquid density based upon pressure was assumed. While the levels shown are not considered very accurate, because of flow effects, it is

a. Break mass flow rate for the two larger breaks (S-SF-1 and S-SF-2) was measured with an upstream-of-break drag screen and densitometer arrangement. Break flow for the smallest break (S-SF-3) was also redundantly measured with a break flow condensing tank. This accounts for the relatively slow rise time shown for the Test S-SF-3 break flow.

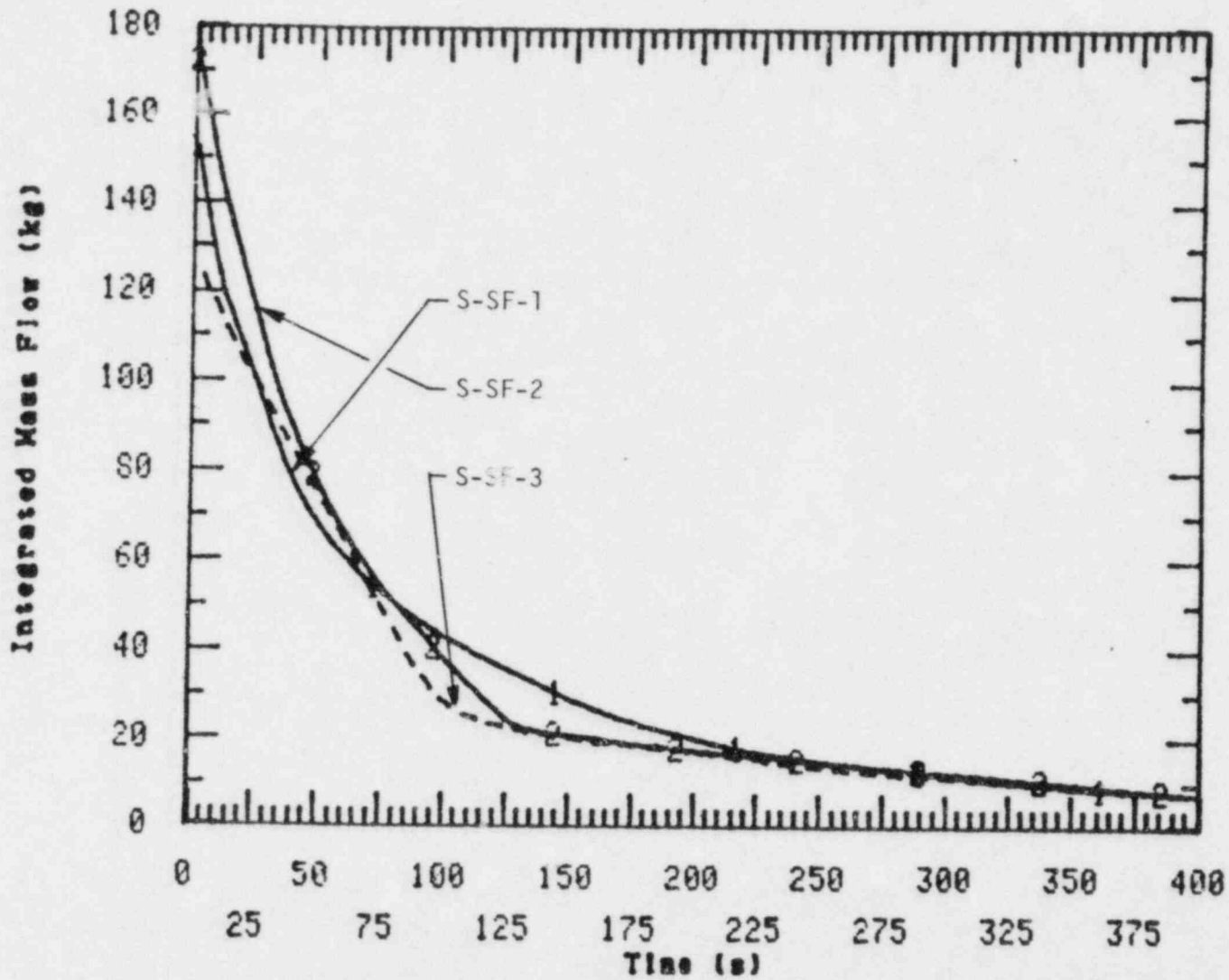


Figure 12. Broken Loop Steam Generator Mass Inventory for Tests S-SF-1, S-SF-2, and S-SF-3.

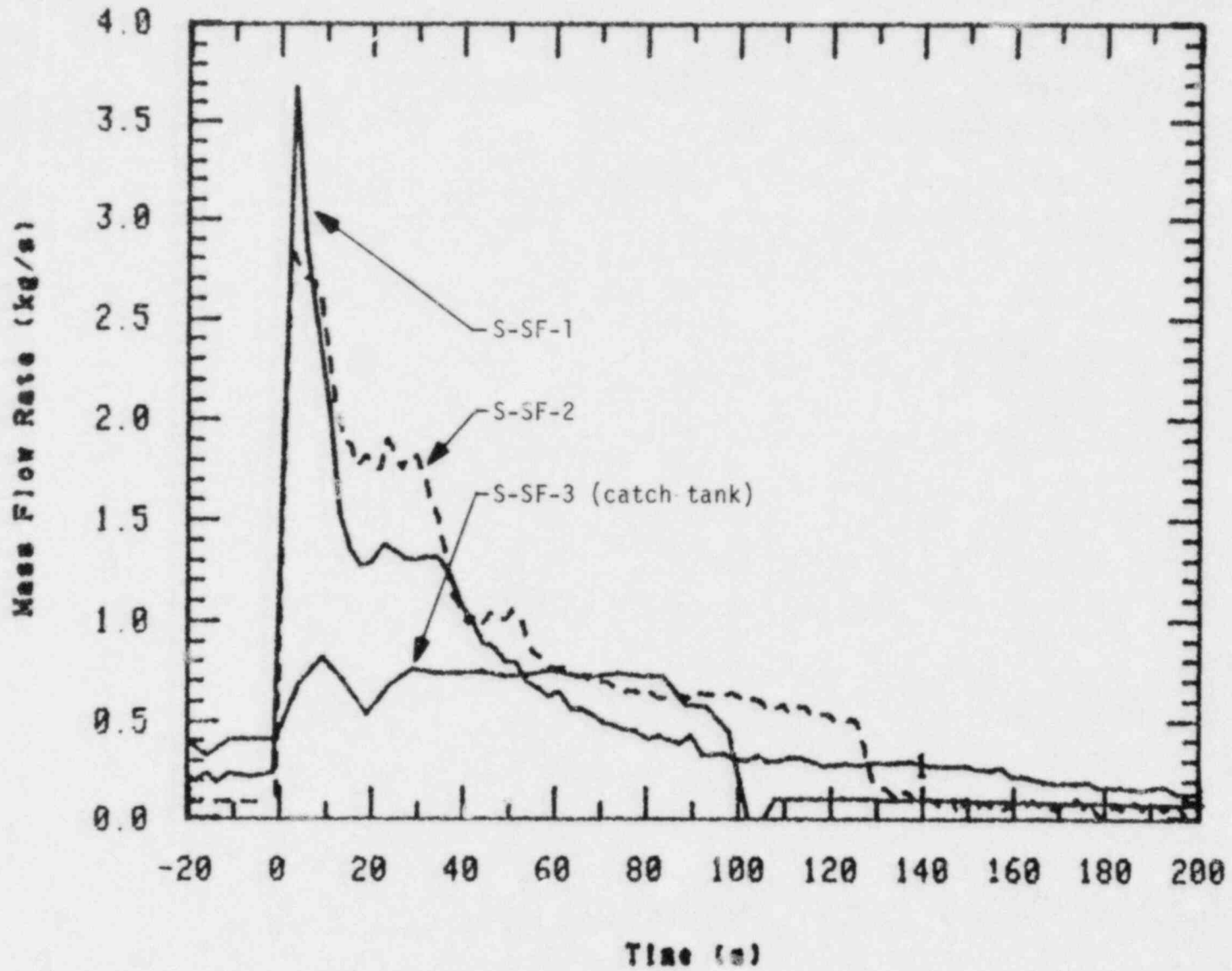


Figure 13. Flow rate from feedwater line break for Tests S-SF-1, S-SF2, and S-SF-3.

1 RSC=FLB1M

2 RSC=FLB1T

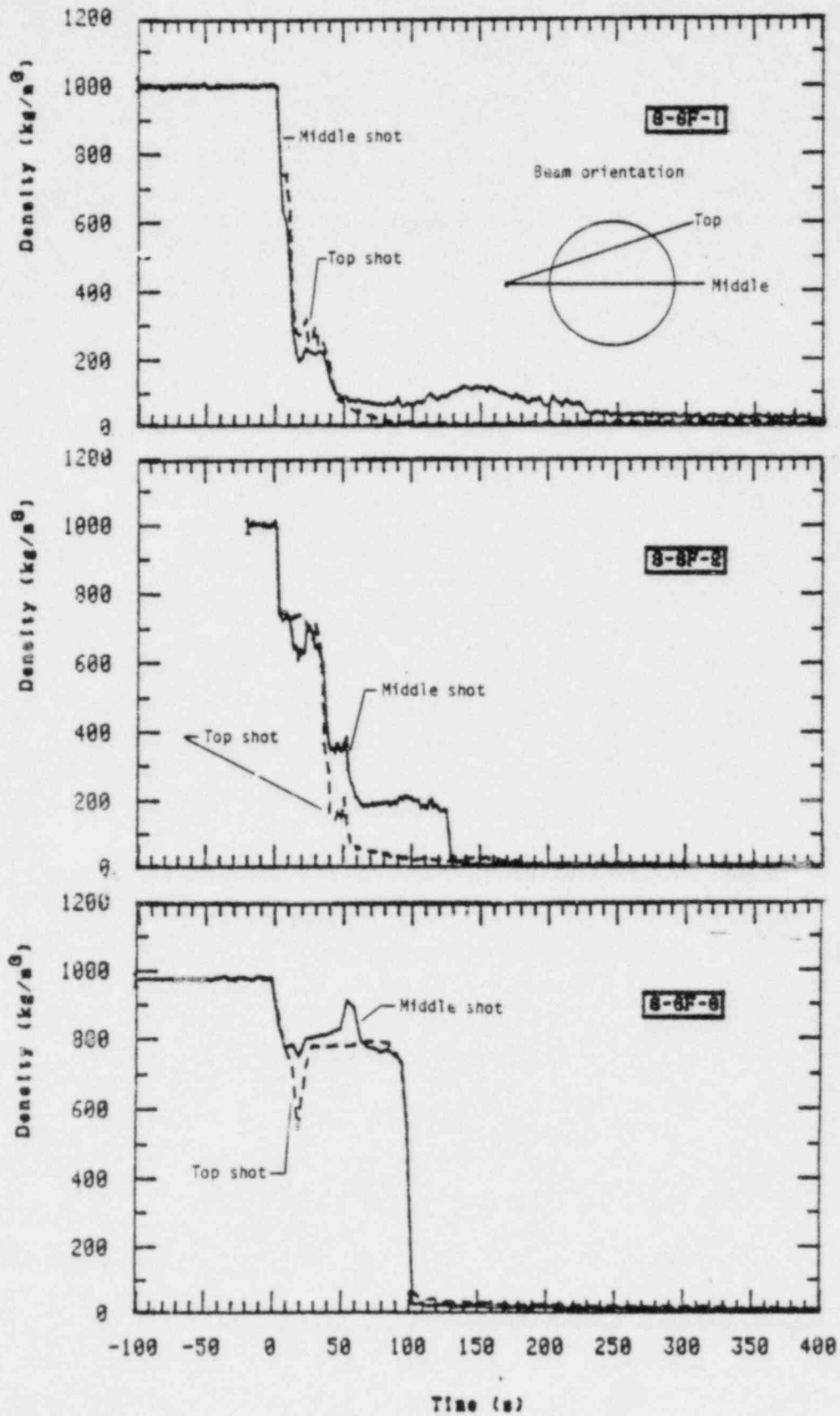


Figure 14. Fluid densities upstream of break for Tests S-SF-1, S-SF-2, and S-SF-3.

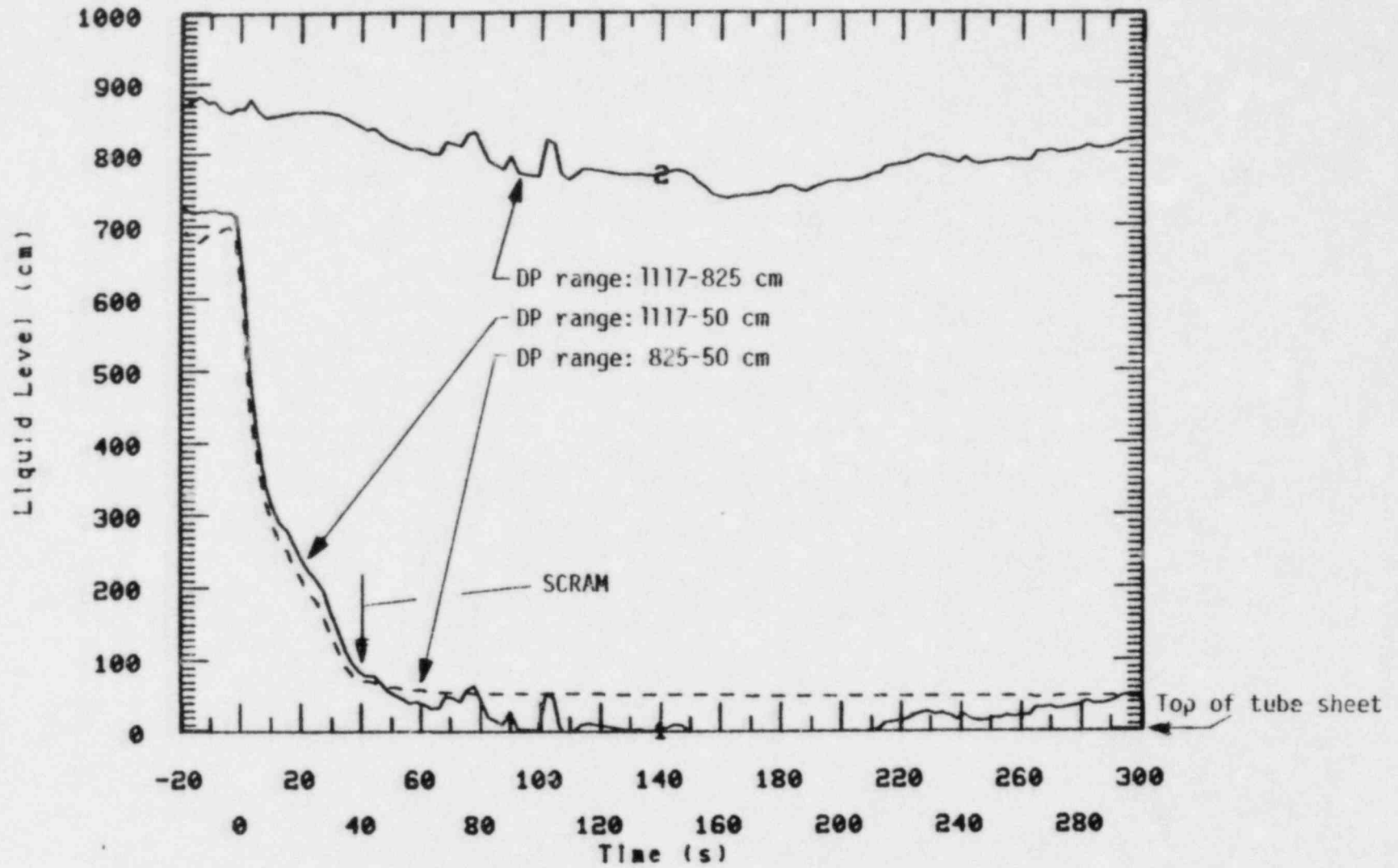


Figure 15. Collapsed liquid levels in the broken loop steam generator for Test S-SF-1.

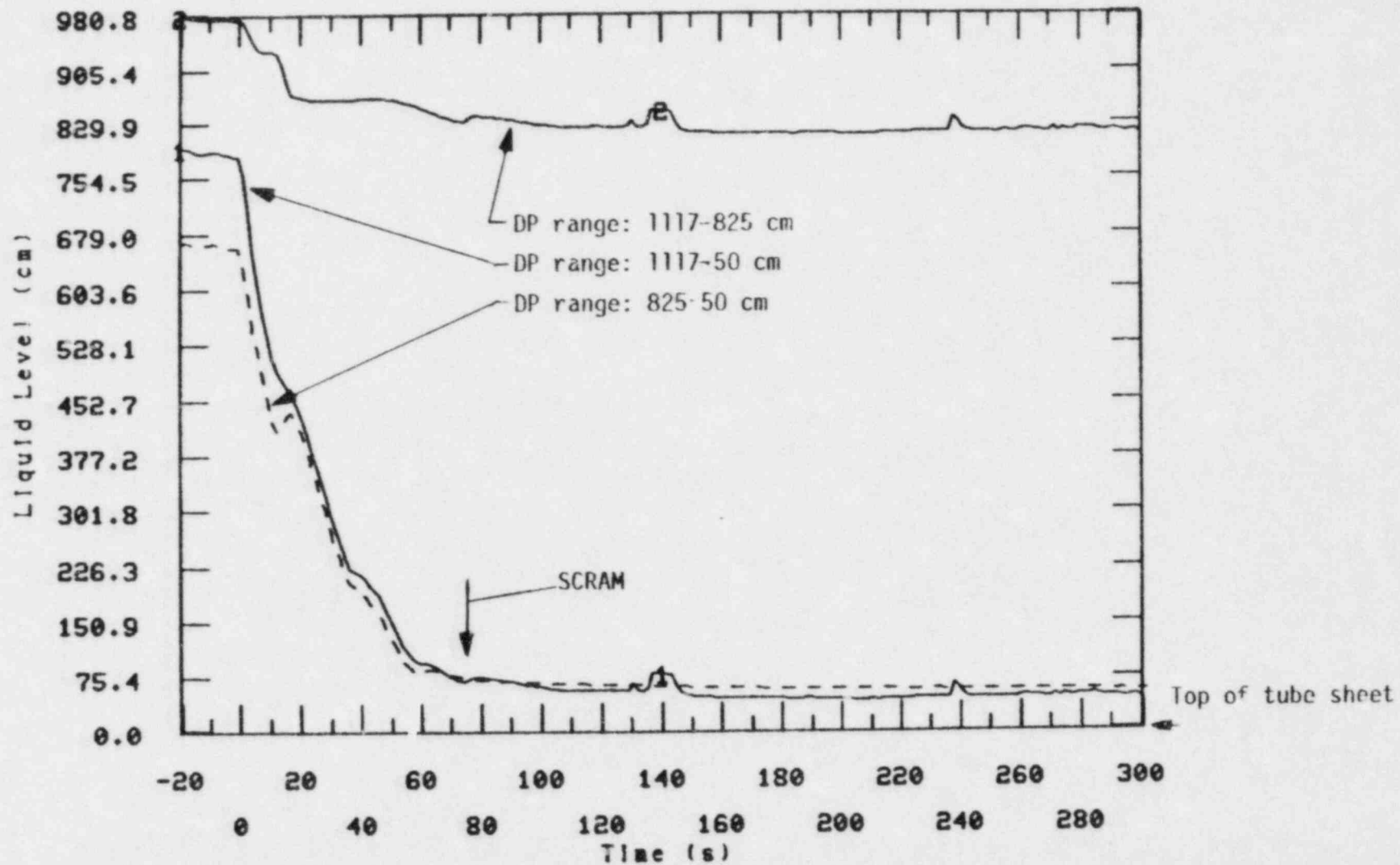


Figure 16. Collapsed liquid levels in the broken loop steam generator for Test S-SF-2.

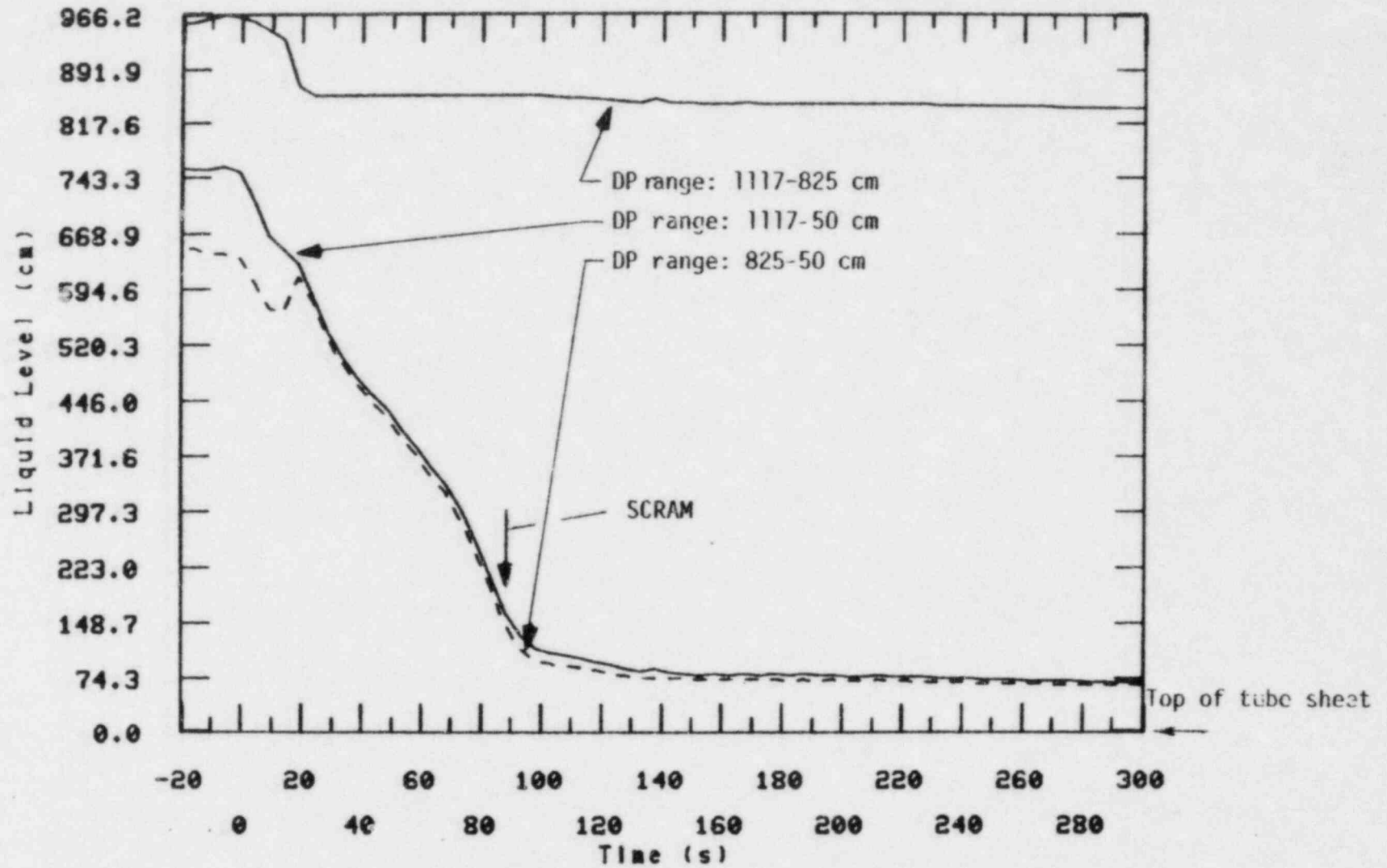


Figure 17. Collapsed liquid levels in the broken loop steam generator for Test S-SF-3.

interesting to note that the indicated levels drop rather rapidly, immediately as the break opens, and the indicated level is extremely low (0 to 10%) when the high primary pressure trip is reached.^a

Figures 18 through 20 show the calculated collapsed liquid levels in the intact loop secondary. Again, no flow corrections have been applied. Because of the large excess amount of water in the broken loop secondary, the blowdown was extended allowing a significant loss of inventory from the intact loop generator prior to isolation. As seen in the figures the collapsed liquid level was about 200 to 300 cm once the steam generator was isolated and flow effects diminished. After isolation the levels are seen to slowly increase due to the injection of auxiliary feedwater.

3.3 Primary Response

In all three tests the primary system pressure underwent a sudden and rapid increase corresponding to loss of secondary heat sink. Figure 21 compares the pressurizer pressure response for the three experiments during the early portion of the transients. The pressure decreased slightly after initiation of the transient in all cases corresponding primarily to termination of pressurizer heating at time zero. The pressurization is then very rapid in all the tests up to the SCRAM setpoint of 15.86 MPa. Some overshoot occurred following receipt of the SCRAM signal and prior to the core power dropping to decay heat levels. As seen in Figure 21 the pressurization rates in Tests S-SF-1 and S-SF-3 were faster than that of Test S-SF-2. The reason for this difference is apparent in Figures 22, 23 and 24, which show the heat loads (primary-to-secondary heat transfer) of the intact and broken loop steam generators overlayed with the respective primary pressures. Refer also to the initial inventory values for the steam generators given in Table 1. For Test S-SF-2, Figure 23 shows that the intact loop heat load remained fairly constant, and even picked up some of the load decrease of the broken loop prior to SCRAM. The pressurization

a. A low secondary side level trip was disallowed for the experiments conducted.

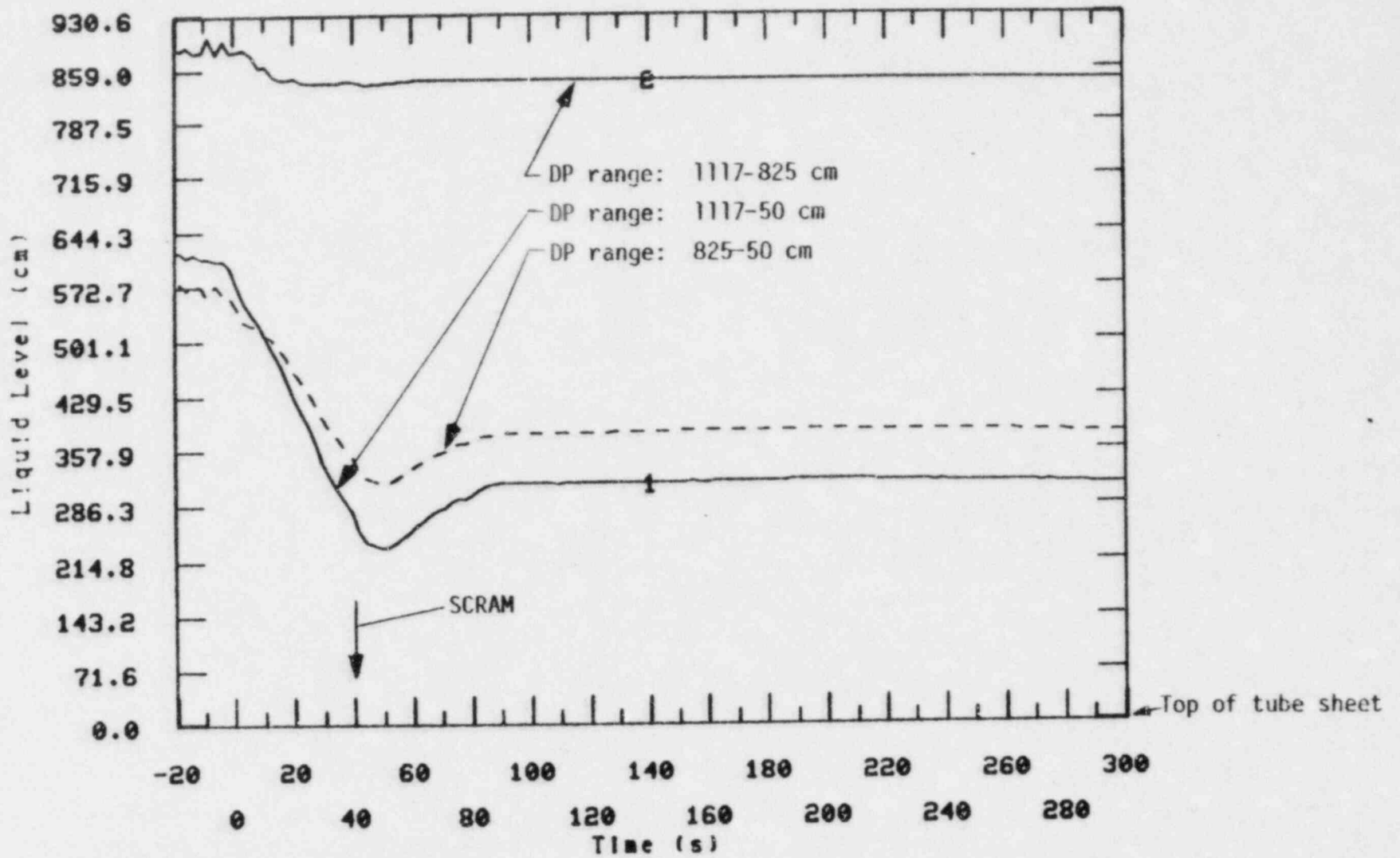


Figure 18. Collapsed liquid levels in the intact loop steam generator for Test S-SF-1.

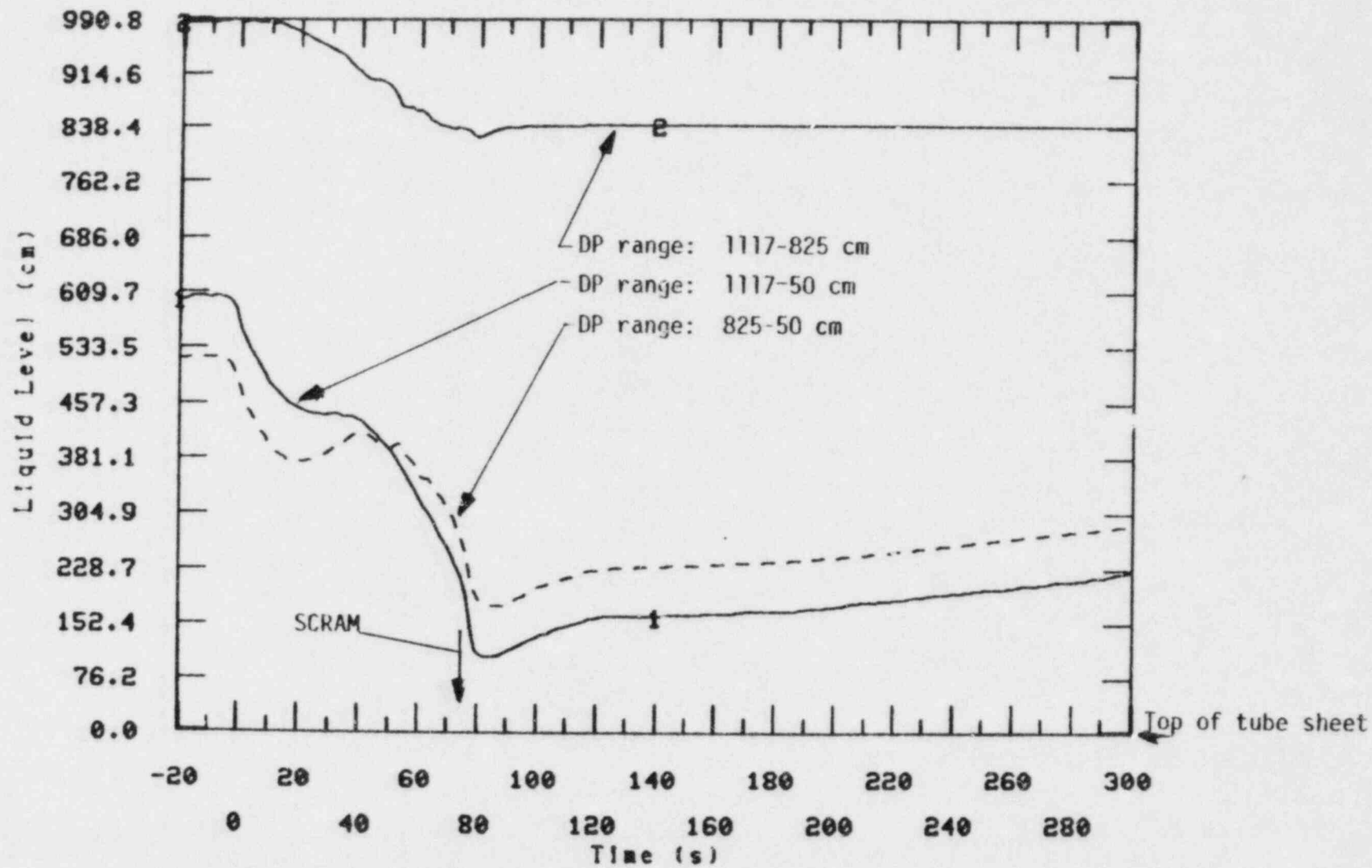


Figure 19. Collapsed liquid levels in the intact loop steam generator for Test S-SF-2.

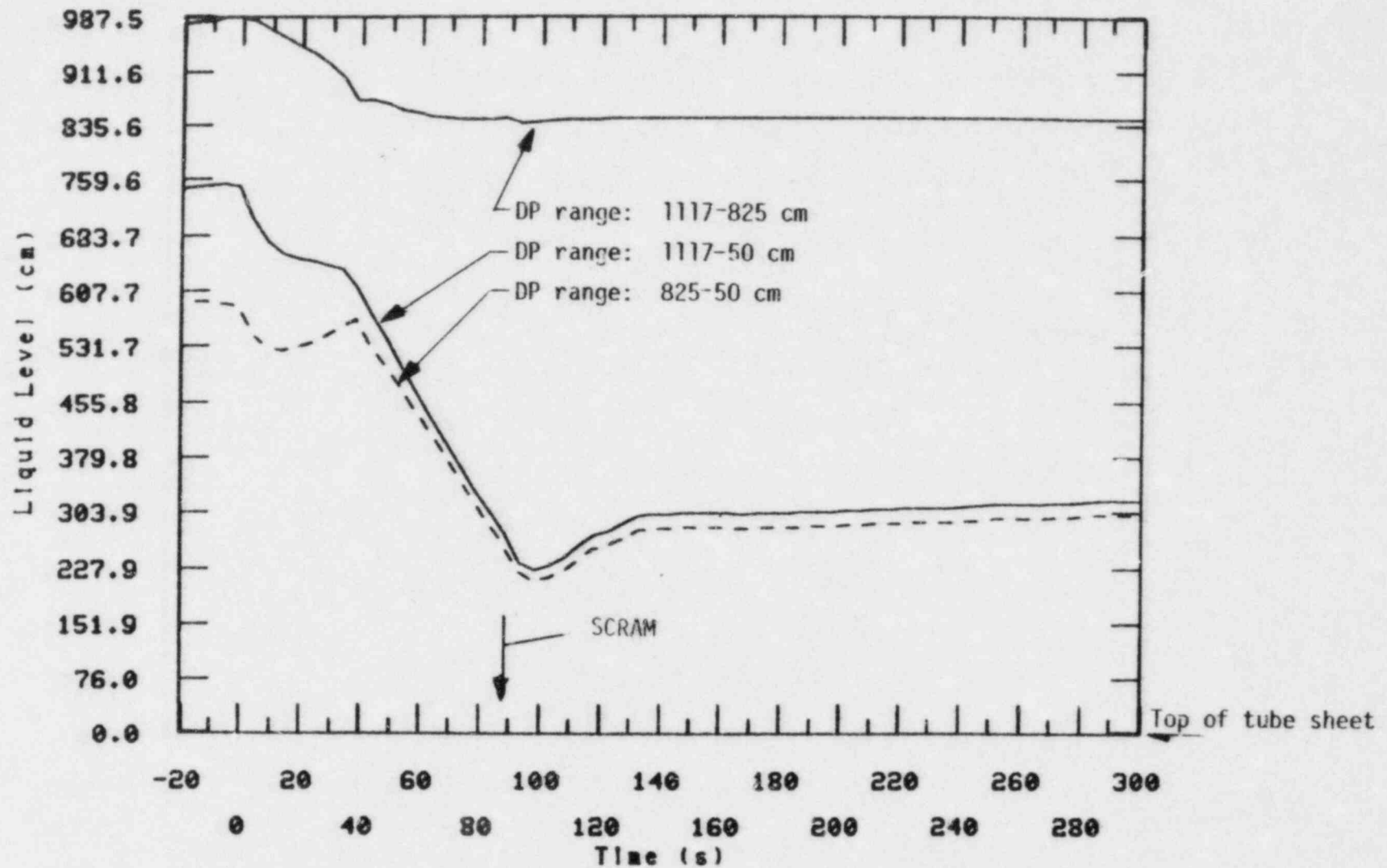


Figure 20. Collapsed liquid levels in the intact loop steam generator for Test S-SF-3.

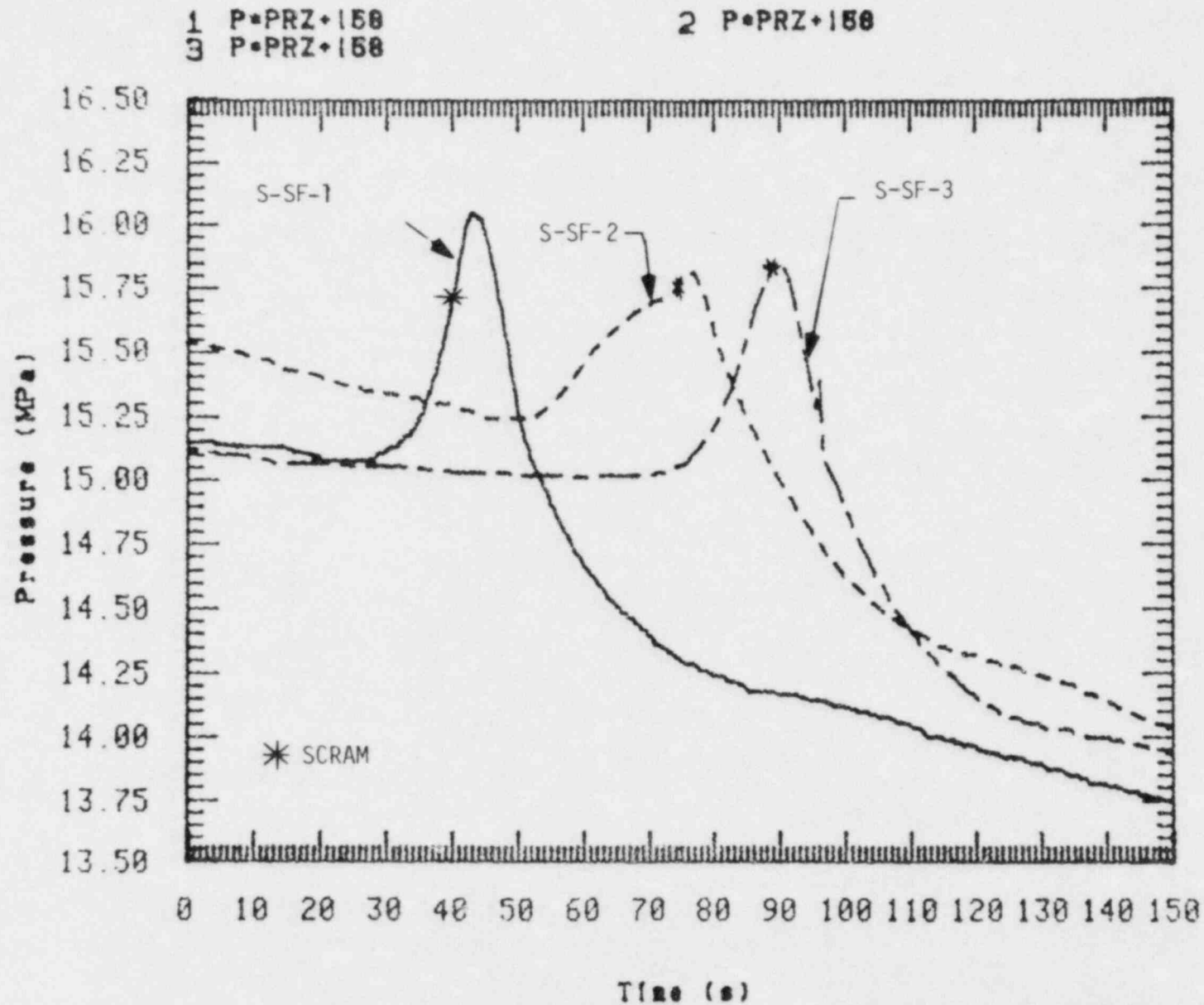


Figure 21. Comparison of primary pressures for Tests S-SF-1, S-SF-2 and S-SF-3.

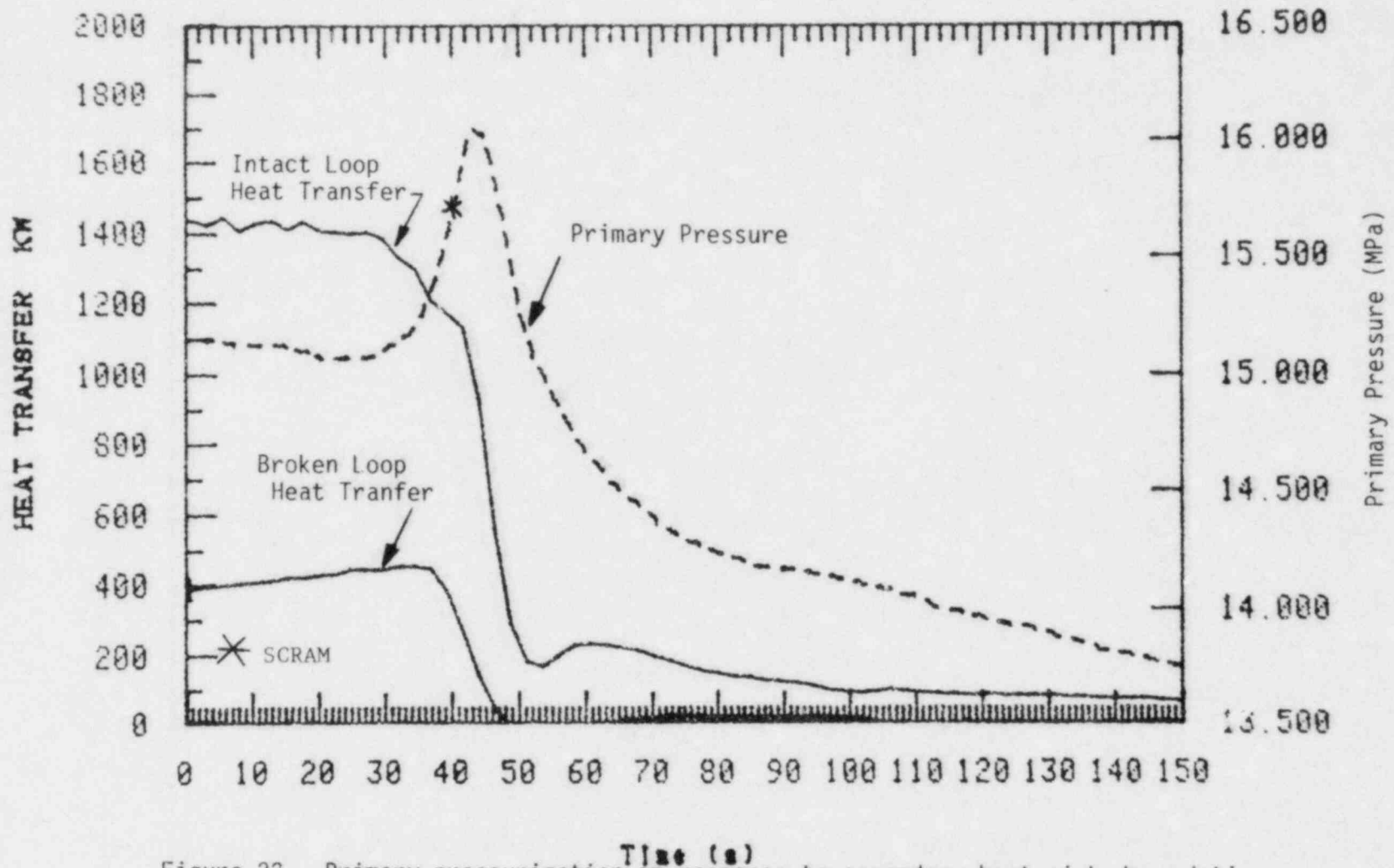


Figure 22. Primary pressurization in response to secondary heat sink degradation, Test S-SF-1.

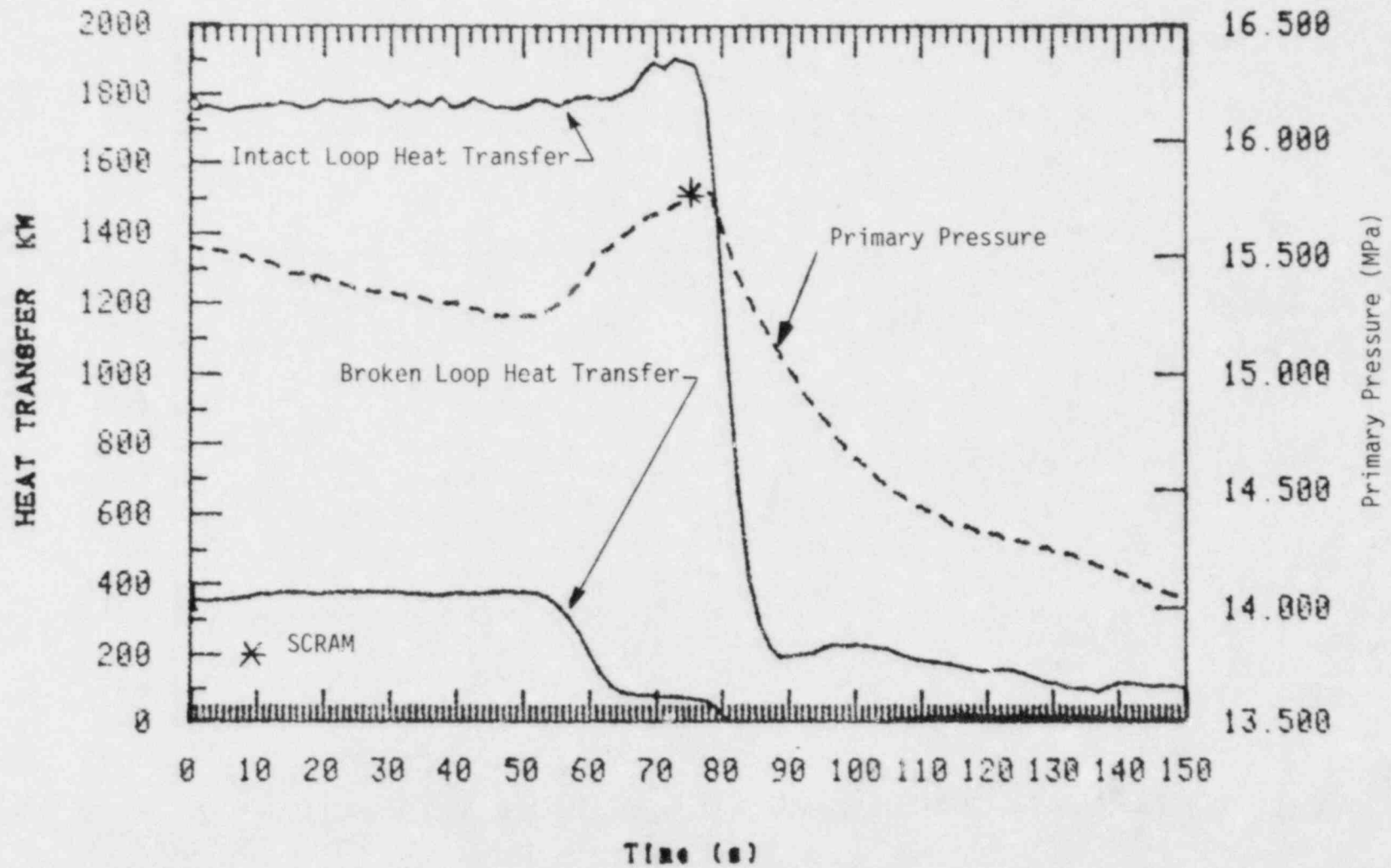


Figure 23. Primary pressurization in response to secondary heat sink degradation, Test S-SF-2.

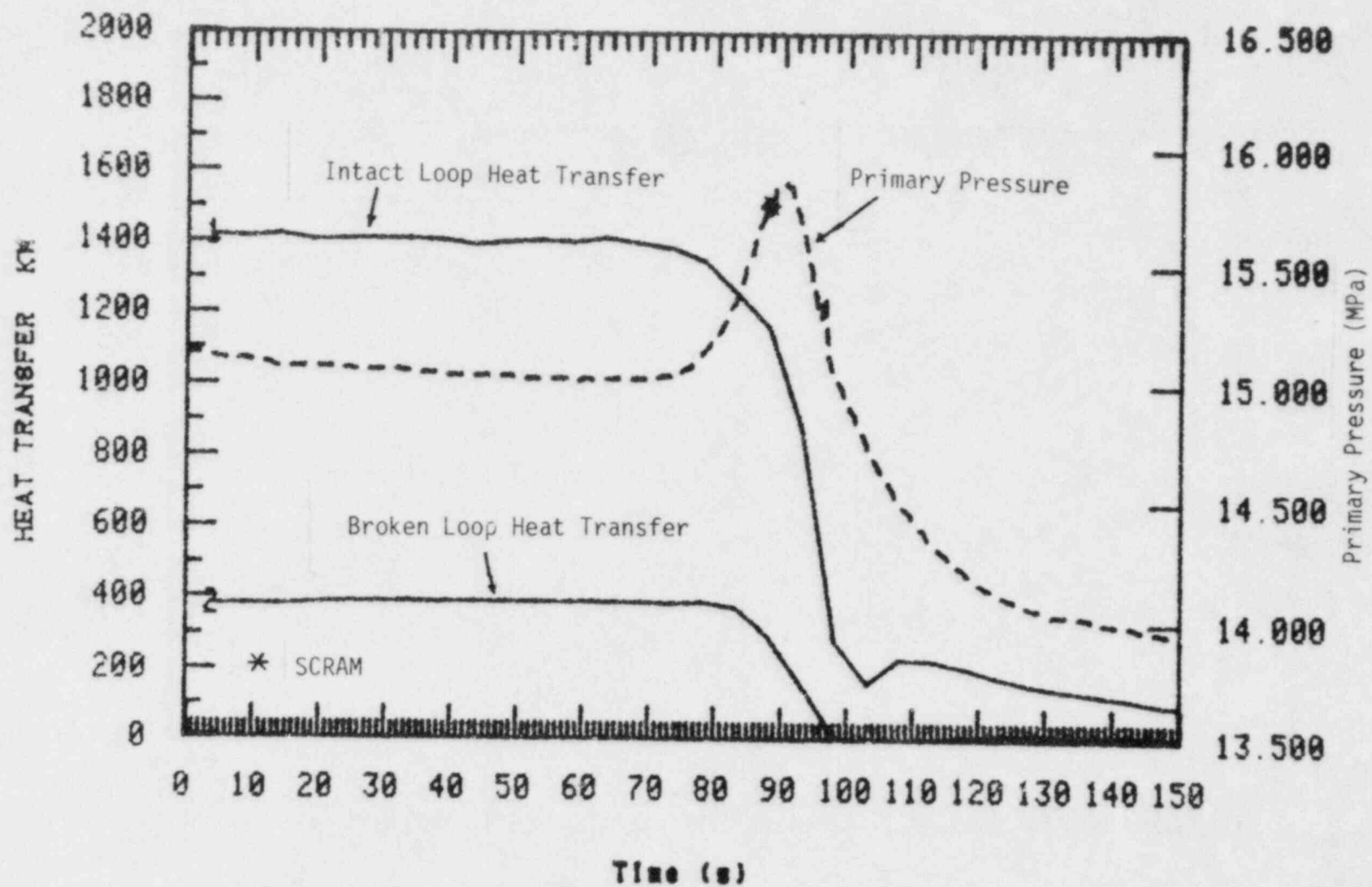


Figure 24. Primary pressurization in response to secondary heat sink degradation, Test S-SF-3.

rate for S-SF-2 therefore reflects only the loss of the broken loop heat sink.^a For Tests S-SF-1 and S-SF-3 the intact loop heat load is seen to have begun decreasing along with the broken loop prior to SCRAM. The pressurization rates for these tests therefore reflect a much larger heat sink reduction, 25% by time of SCRAM in Test S-SF-1 and 32% in Test S-SF-3.

The reason for the relatively earlier loss of intact loop heat sink in Tests S-SF-1 and 3 is partly the result of initial secondary inventory differences between the three experiments, coupled with the heat transfer versus inventory break size dependence discussed in the following section. The ratios of broken loop to intact loop initial secondary masses were 2.02, 1.73, and 1.1 for, respectively, Tests S-SF-1, S-SF-2, and S-SF-3. In terms of inventories, the smaller the ratio the more mass left in the intact loop at isolation, and correspondingly less degradation of heat sink capability. But this is tempered by a loss of broken loop sink at lower inventories with decreasing break size which acts to shift the time of the isolation. The net results are the transient timing behaviors described above, wherein only in Test S-SF-2 did enough inventory remain in the intact loop steam generator throughout the blowdown to maintain adequate heat rejection.

Figure 25 shows the pressurizer collapsed liquid level behavior for the experiments. Figure 26 compares the differential pressure across the pressurizer surge line and Figure 27 shows the pressure in the broken loop cold leg near the pump outlet (system high pressure point). Once the secondary heat sink is lost the heat up and expansion of the primary fluid produces a rapid insurge of fluid into the pressurizer. The pressure in the primary system exceeds that of the pressurizer by an amount determined by the surge line hydraulic resistance and the rapidness of the insurge. The increase in pressurizer pressure for Tests S-SF-1 and S-SF-2, with only

a. Another point worth noting from Figures 22 through 24 is that the broken loop was only rejecting approximately 20% of the core power at initial conditions, rather than the correctly scaled 25%. This came about because of errors in the process instrumentation which is used to control the system and establish initial flows and ΔT s.

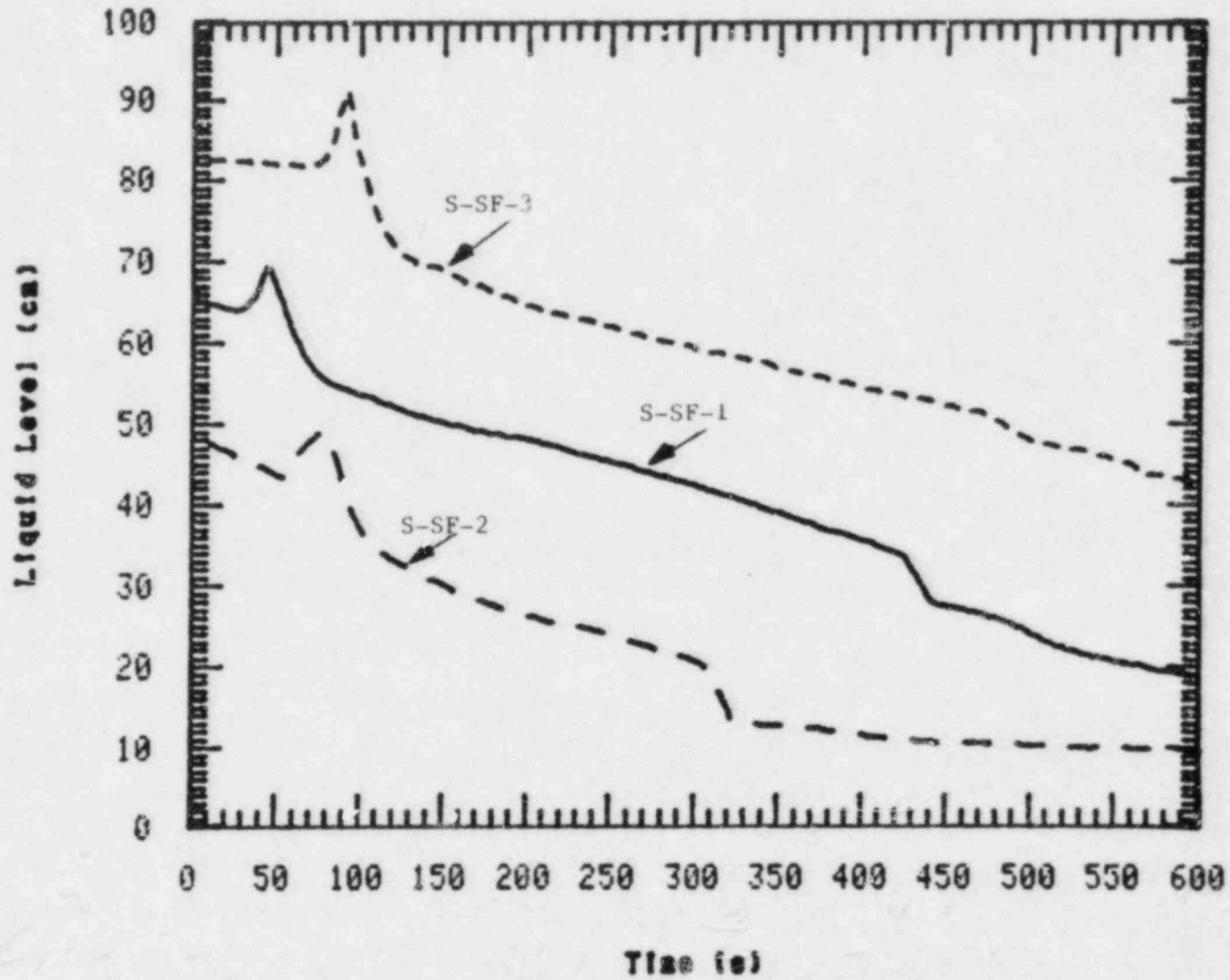


Figure 25. Collapsed liquid levels in the pressurizer as calculated with saturated liquid density. (S-SF-2 data has been adjusted to compensate for instrument offset.)

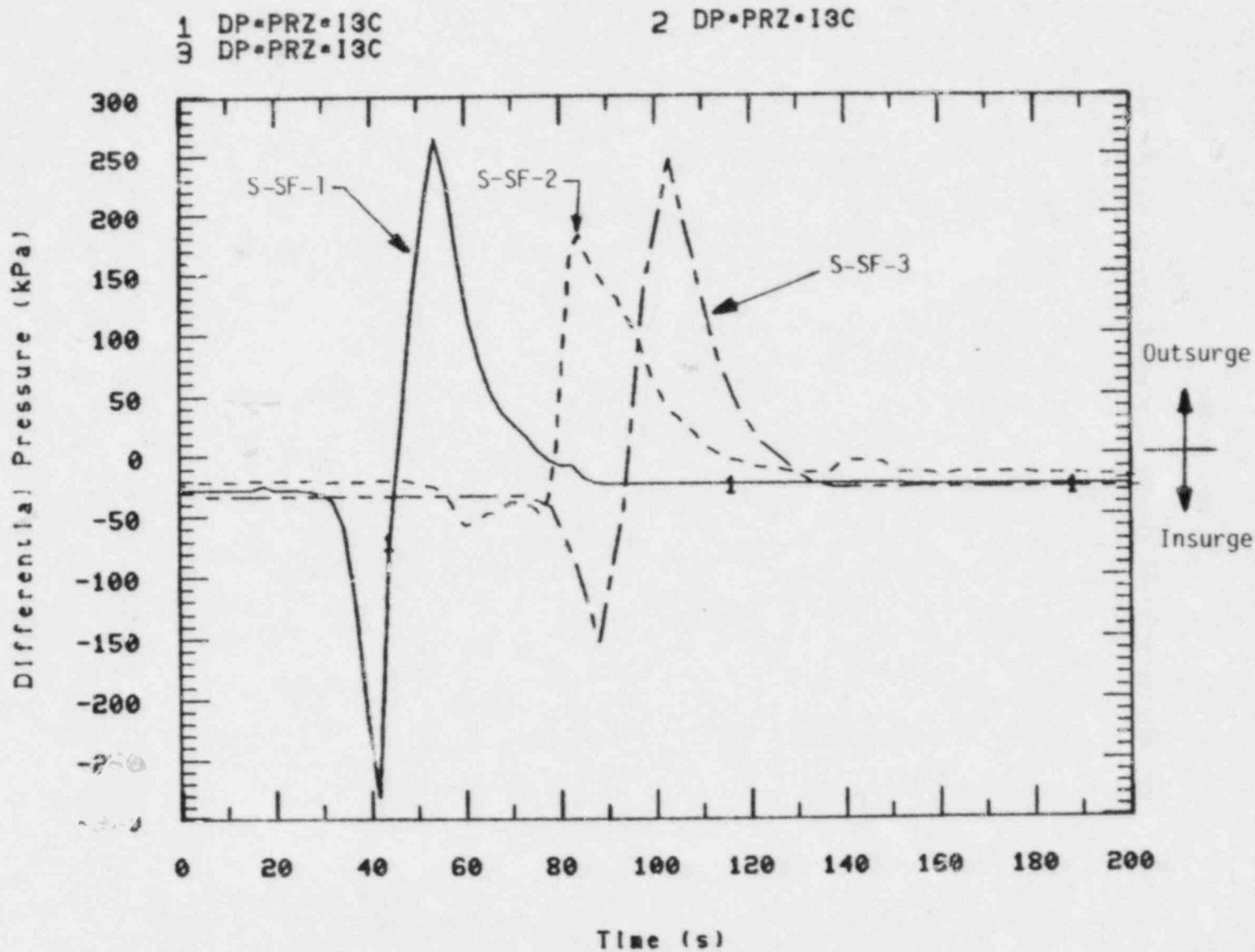


Figure 26. Pressurizer surge line differential pressure during secondary blowdown for Tests, S-SF-1, S-SF-2, and S-SF-3.

1 PB-79
3 PB-79

2 PB-79

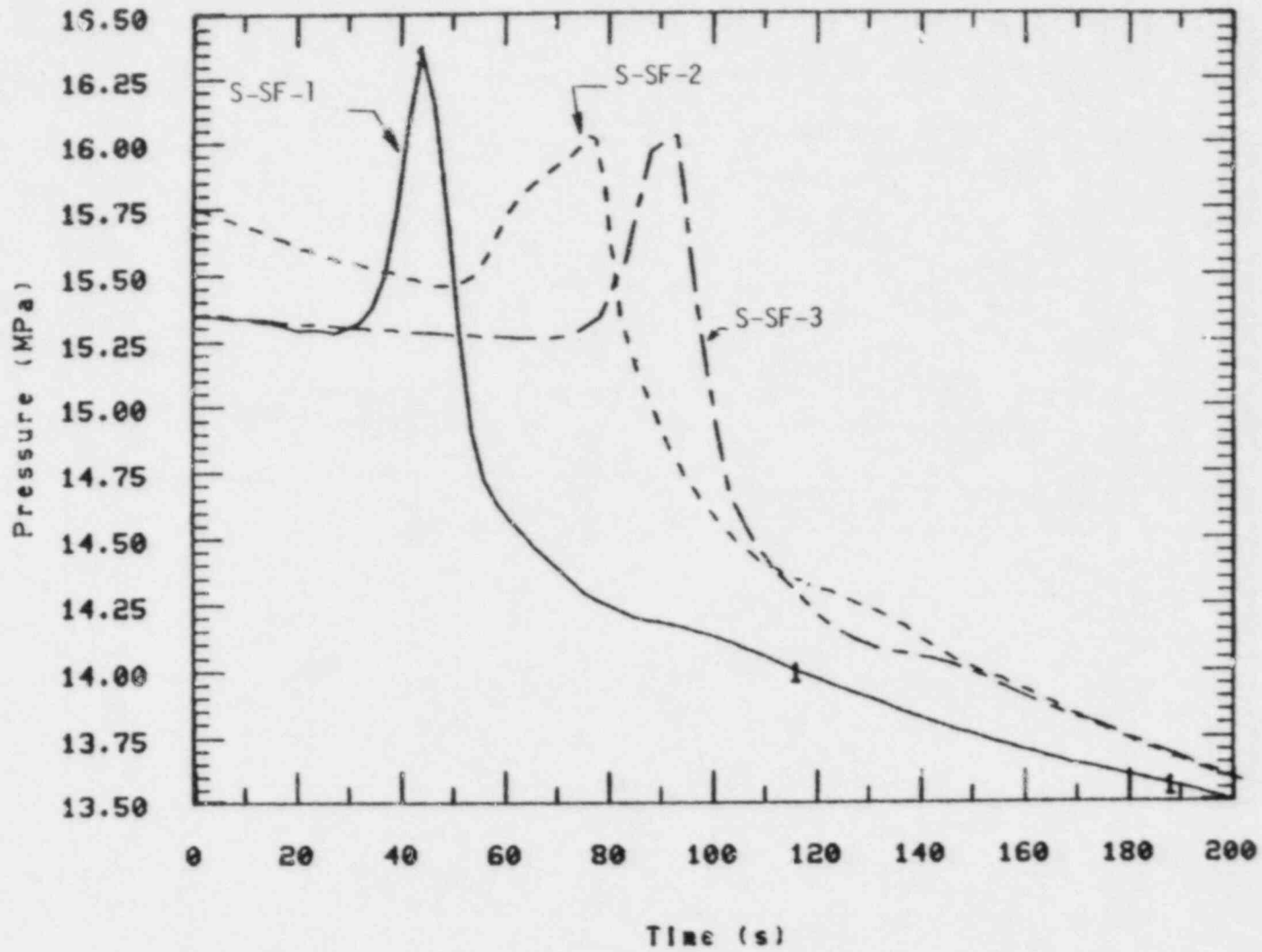


Figure 27. Static pressure downstream of the broken loop pump.

about a 5 cm change in liquid level, approximates a near adiabatic compression of the pressurizer vapor bubble. The pressurization for Test S-SF-3 was less so, although reasons for this are not understood at this time.

Once the core was SCRAMed a rapid shrinkage of the primary inventory occurred and the pressurizer level is seen to have dropped rapidly as liquid flowed into the primary. Due to the continued injection of cold secondary auxiliary feedwater, heat losses to the environment, cold HPIS liquid injection, and primary leakage^a the level continued to decrease until the HPIS injection rate was increased to recover the system. In all tests a rapid level drop occurs as the collapsed level drops into the lower third of the pressurizer due to an abrupt area reduction. This in turn resulted in the sharp pressure drops seen in Figure 10.

As seen in Figures 28, 29 and 30 for each experiment the upper plenum fluid eventually saturated, followed by the upper head fluid. The collapsed liquid levels for the upper plenum and upper head are shown in Figures 31, 32, and 33. Significant voiding occurred in all of the experiments. The extreme voiding seen in Test S-SF-3 was induced by continued primary bleeding without HPIS injection in preparation for an attempted primary feed and bleed. Once substantial voiding was observed the HPIS flow rate was increased to speed recovery of the system.^b In Test S-SF-1 the pressurizer liquid level was reestablished, and as soon as the pressurizer heaters were turned back on the voids in the vessel upper plenum and upper head rapidly collapsed.

a. The leak rates at initial conditions for the three tests and the total leakage collected from the primary pump were as follows:

Test	S-SF-1	S-SF-2	S-SF-3
Leak rate (kg/s)	0.005	0.008	0.005
Total pump leakage (kg)	9	12 (estimate)	9.6
Test duration (s)	2100	1450	4500

b. Semiscale natural circulation experiments had already shown that adequate decay heat rejection is possible at primary inventories as low as 50% as long as there is a secondary heat sink.

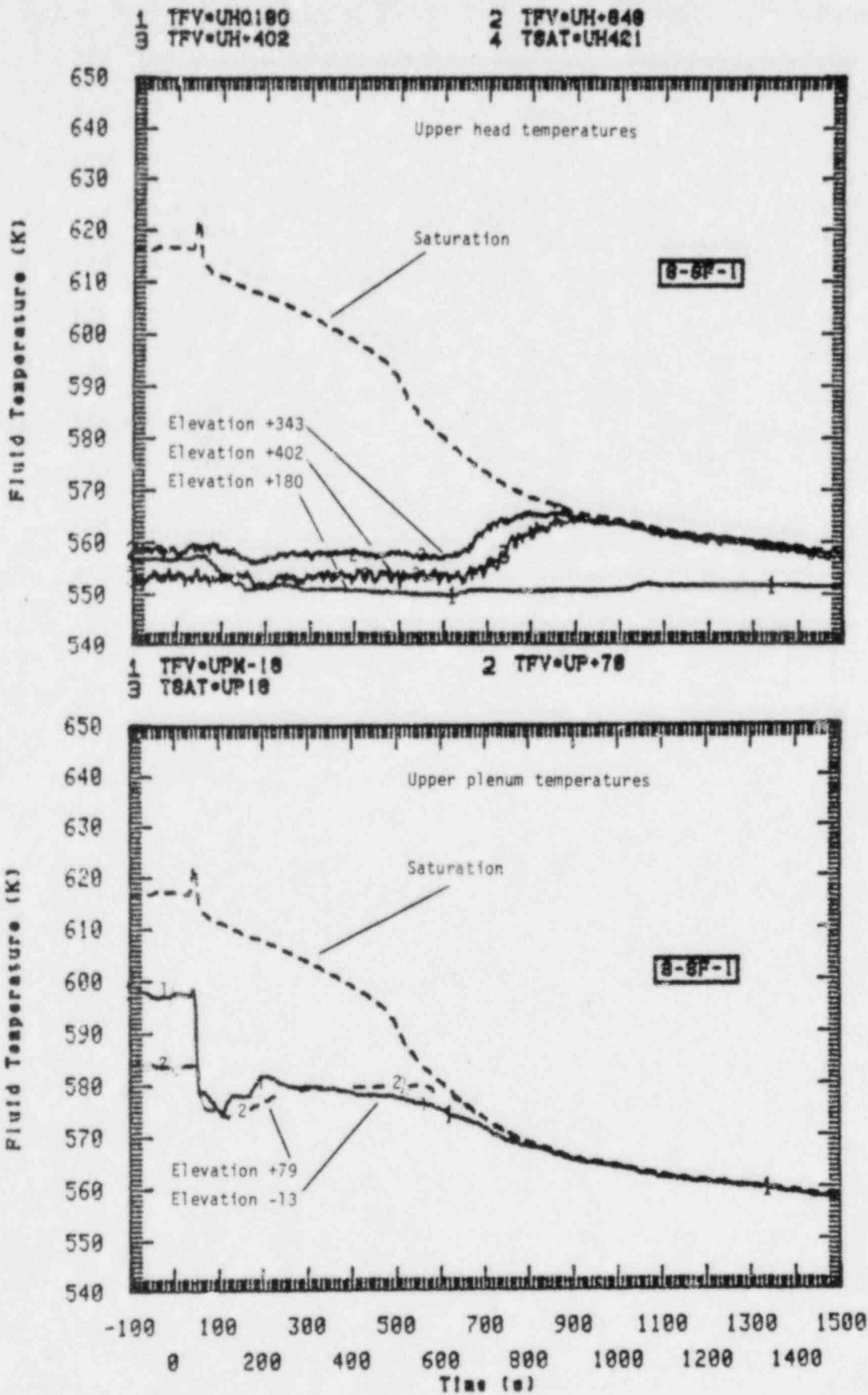


Figure 28. Upper head and upper plenum temperatures for Test S-SF-1.

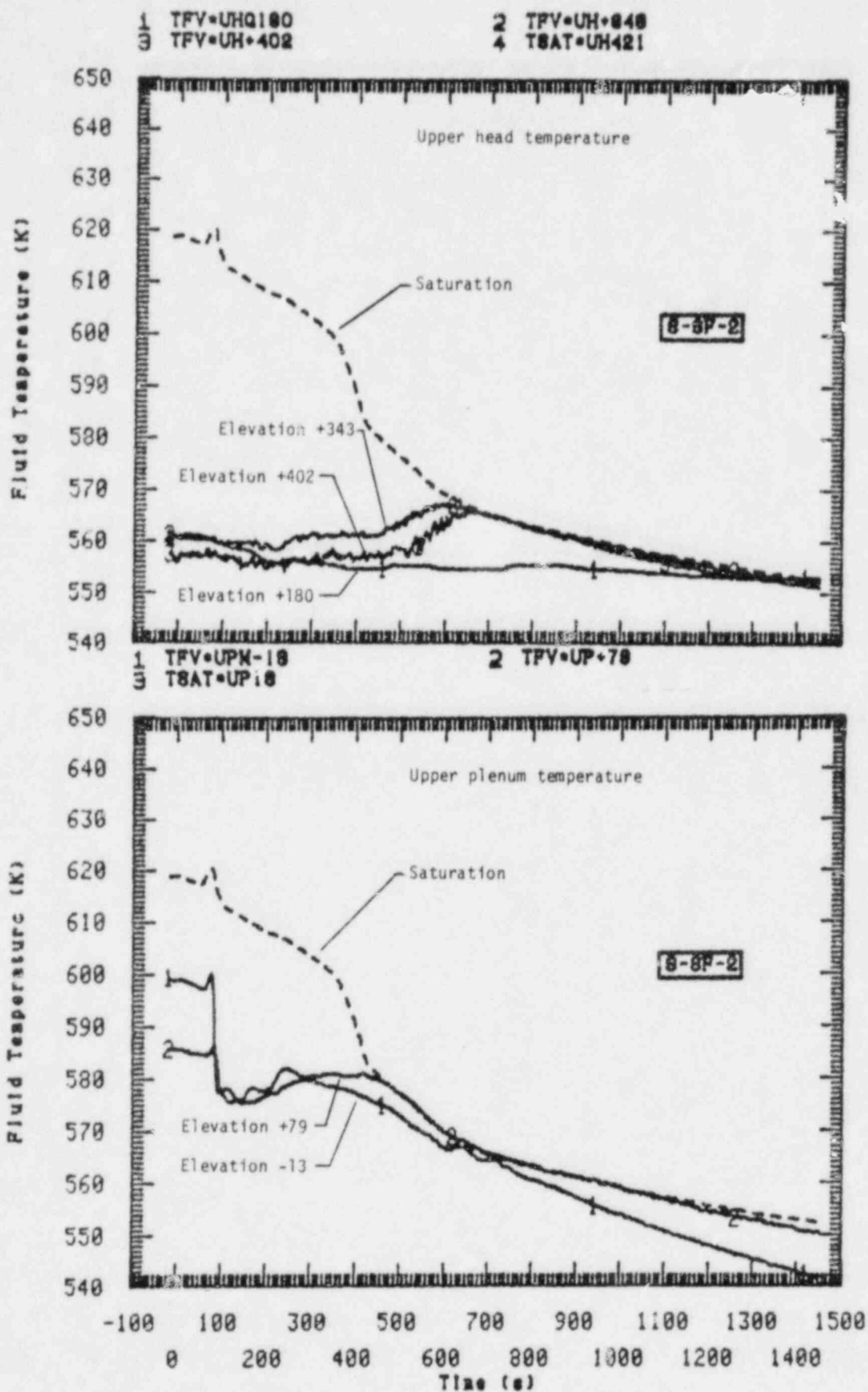


Figure 29. Upper head and upper plenum temperatures for Test S-SF-2.

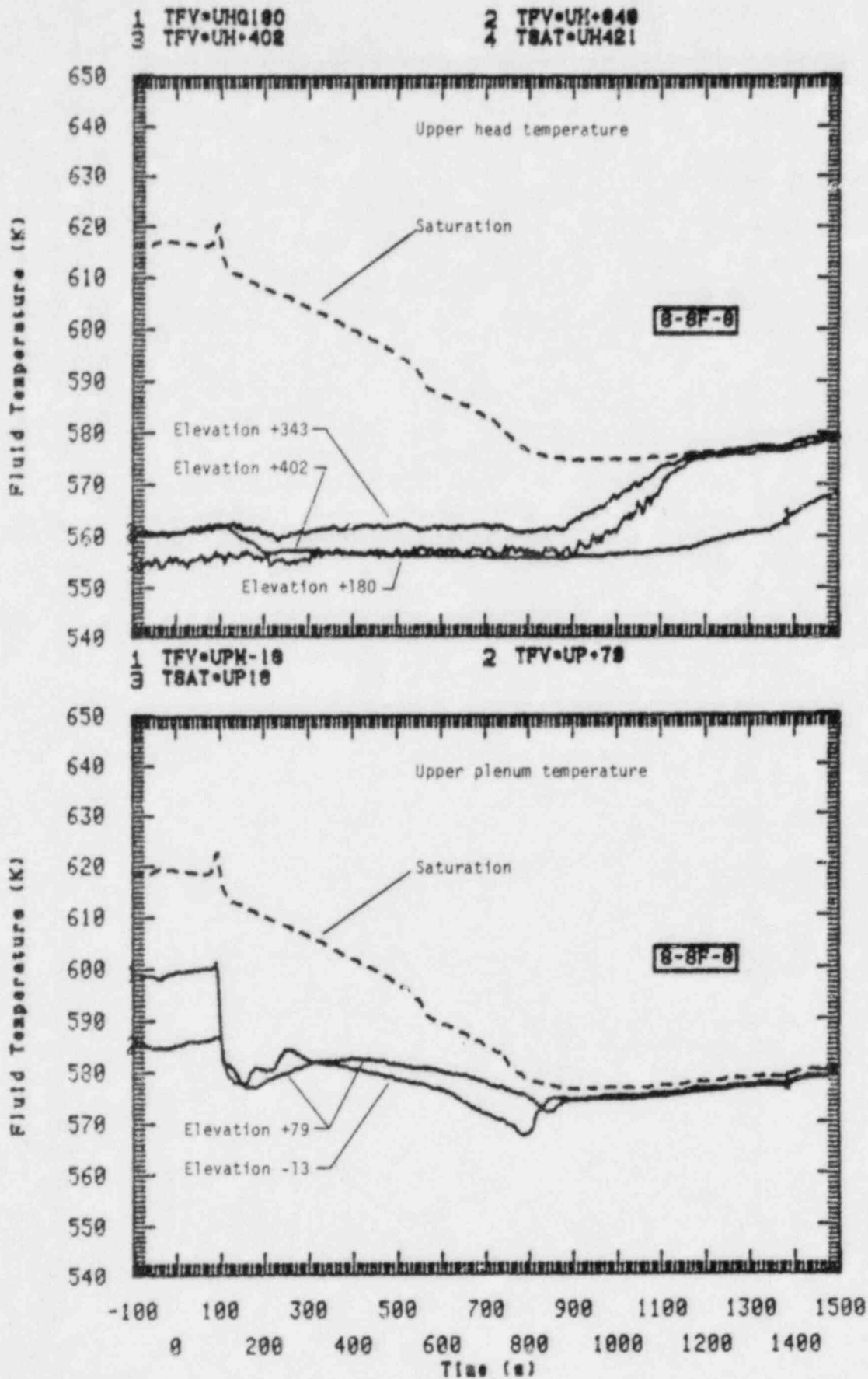


Figure 30. Upper head and upper plenum temperatures for Test S-SF-3.

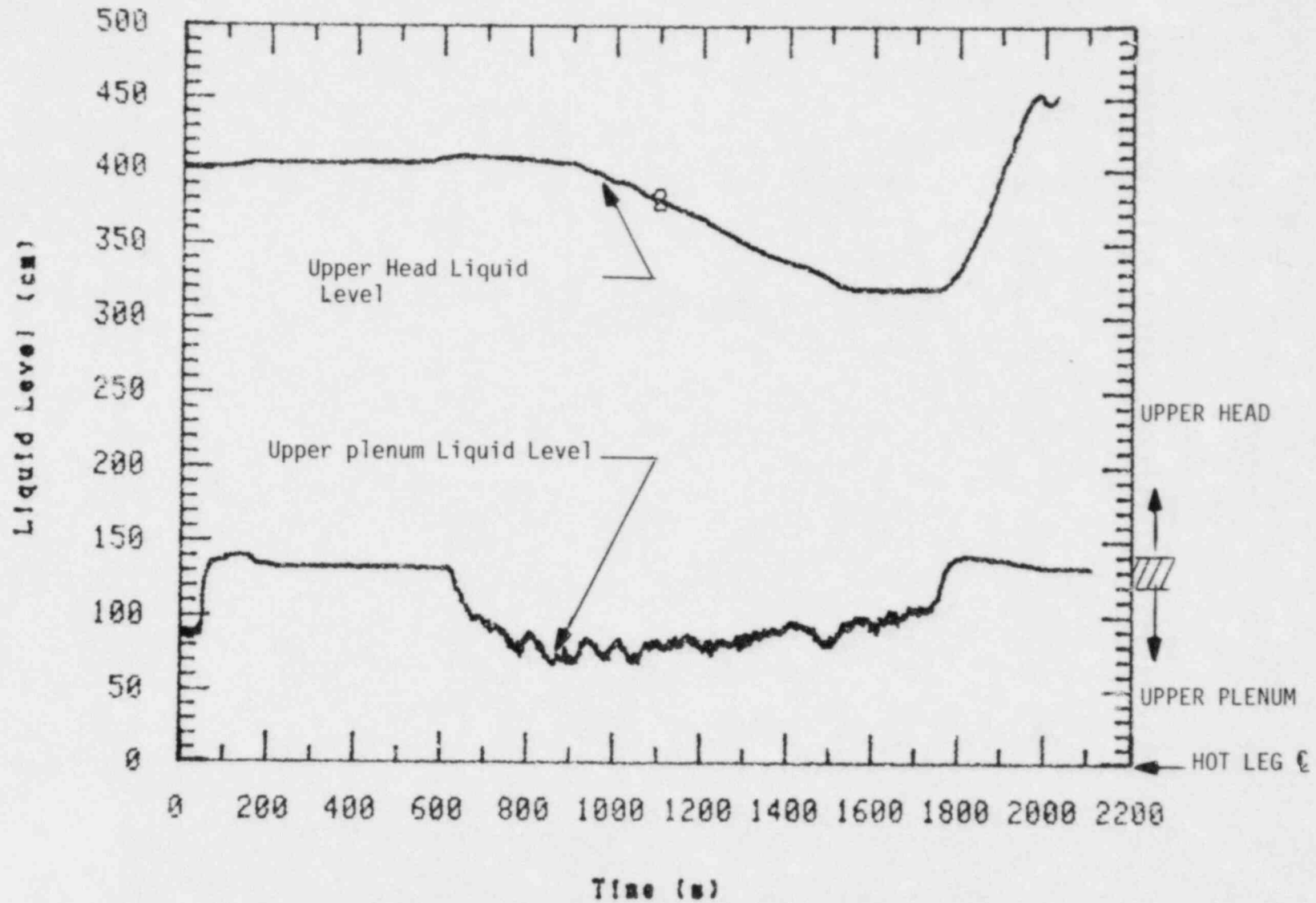


Figure 31. Upper head and upper plenum collapsed liquid levels from hot leg centerline, Test S-SF-1.

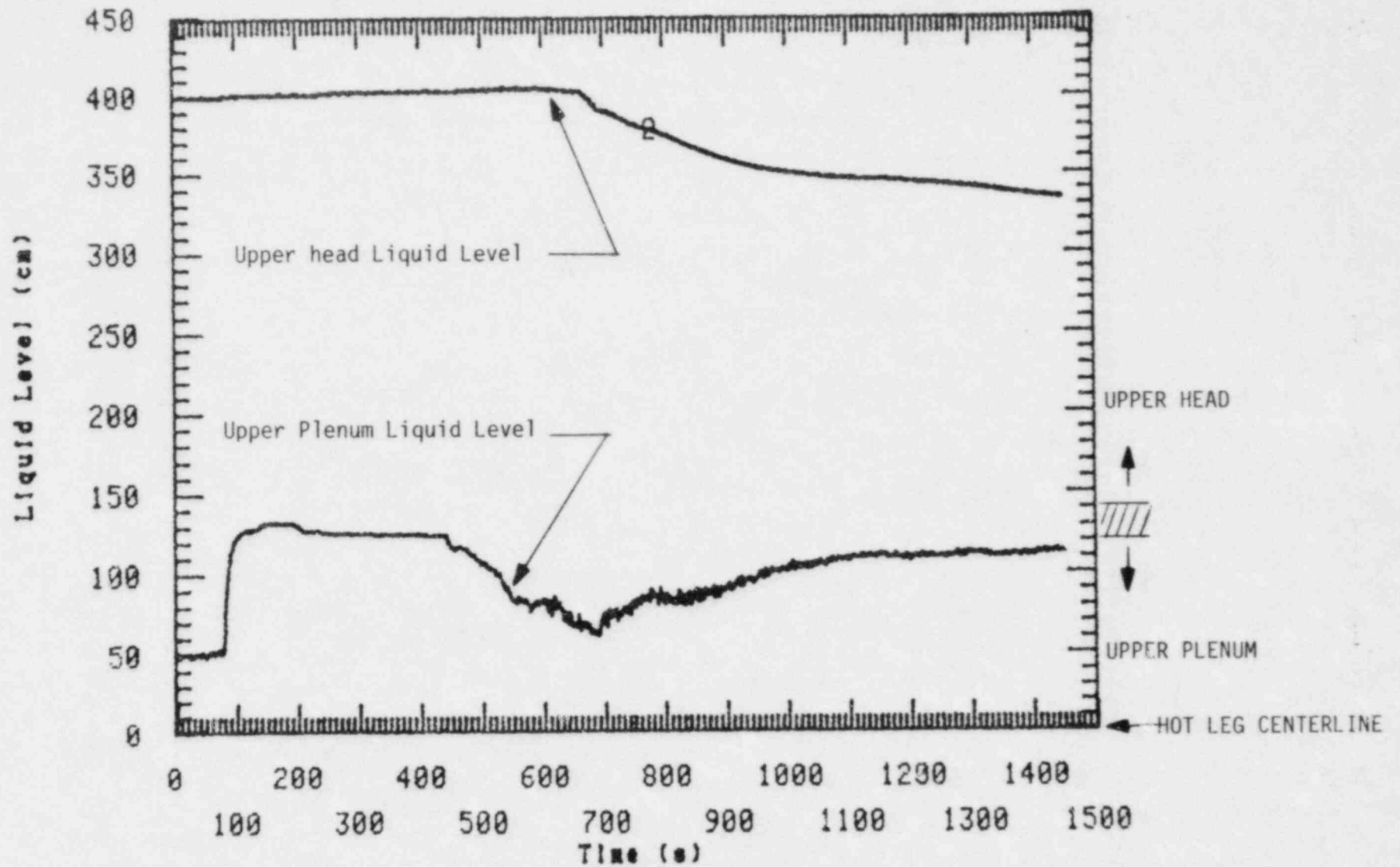


Figure 32. Upper head and upper plenum collapsed liquid levels from hot leg centerline, Test S-SF-2.

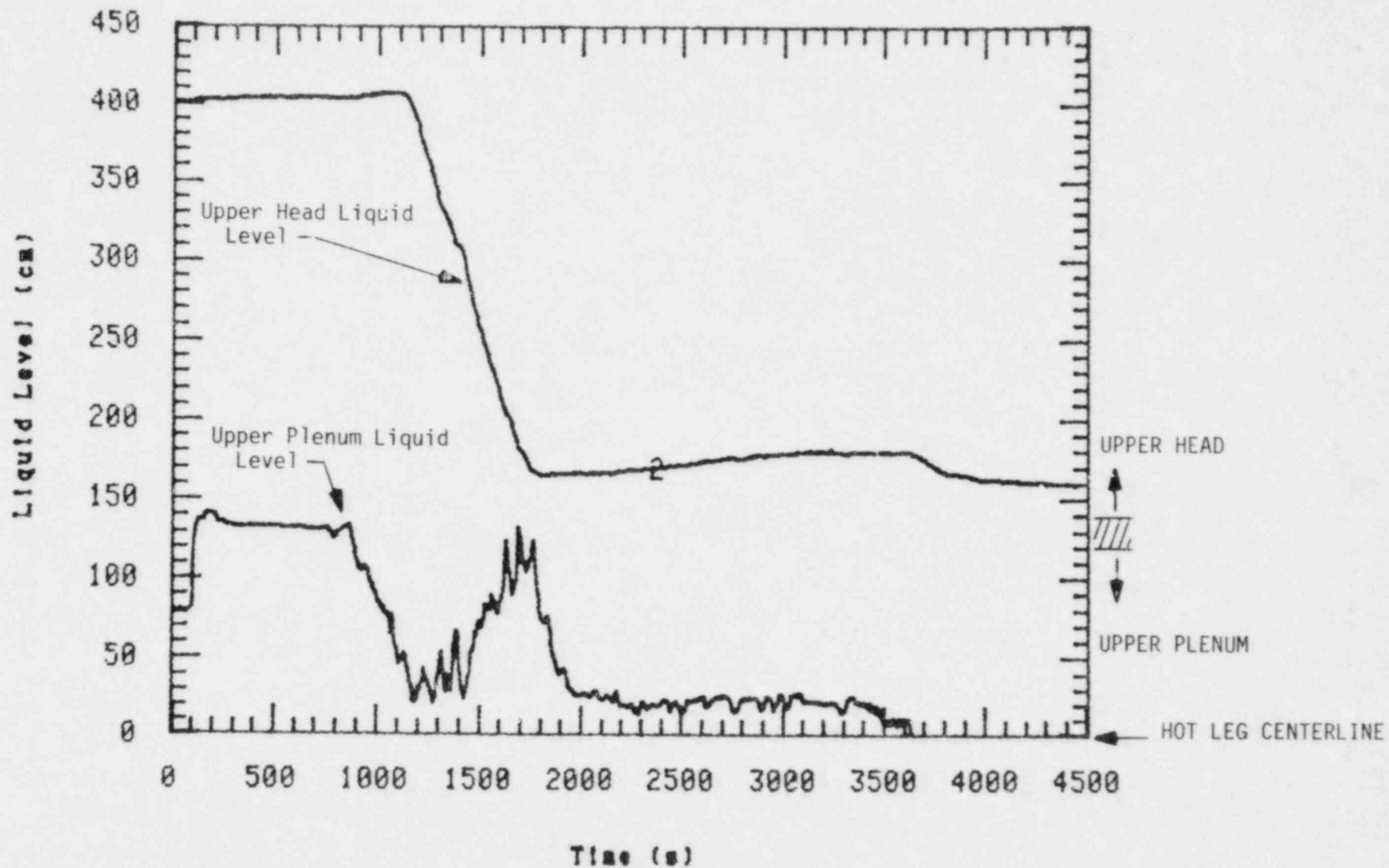


Figure 33. Upper head and upper plenum collapsed liquid levels from hot leg centerline, Test S-SF-3.

3.4 Primary-to-Secondary Heat Transfer

The primary objective of the Semiscale feedwater line break experiments was to evaluate the primary-to-secondary heat transfer behavior. Figure 34 shows the normalized heat transfer to the broken loop steam generator plotted against a normalized inventory.^a Two points are especially notable in regard to the relationship indicated. The first is the rapid drop in heat transfer over a very narrow inventory range. The second is the fact that the heat transfer degrades when there are still substantial quantities of water in the secondary, and at inventories that appear to be break size dependent. This behavior strongly suggests that the degradation in heat transfer is not caused predominantly by the loss of inventory, but rather by a change in the hydraulic conditions at the tube surface, such as large increases in quality. The primary side fluid remained single-phase throughout the blowdown portion of the transients.

Figure 35 shows the temperature behavior at a mid-level location in the broken loop steam generator (452 cm above the tube sheet) as measured by a primary fluid TC, a tube metal TC, and a secondary fluid TC. It can be seen that there is a rapid degradation in the heat transfer coefficient on the outside of the tube that causes the primary fluid and tube metal temperature to converge. There is also enough secondary liquid remaining to keep the secondary fluid thermocouple wetted at saturation temperature. If the secondary inventory at a given location was depleted, the secondary fluid thermocouple would begin to indicate temperatures at, or approaching, the primary temperature. This is seen to be the case in Test S-SF-3, which depleted to the lowest inventory, immediately following the SCRAM when the two-phase level collapses.

Figure 36 shows selected "local" heat transfer rates. These were calculated by taking the difference between available primary fluid

a. The heat loads were taken to be 100% at initial conditions for each individual test. The inventories were all normalized to the collapsed secondary liquid volume below the top of the tubes at 6.5 MPa (94.5 kg).

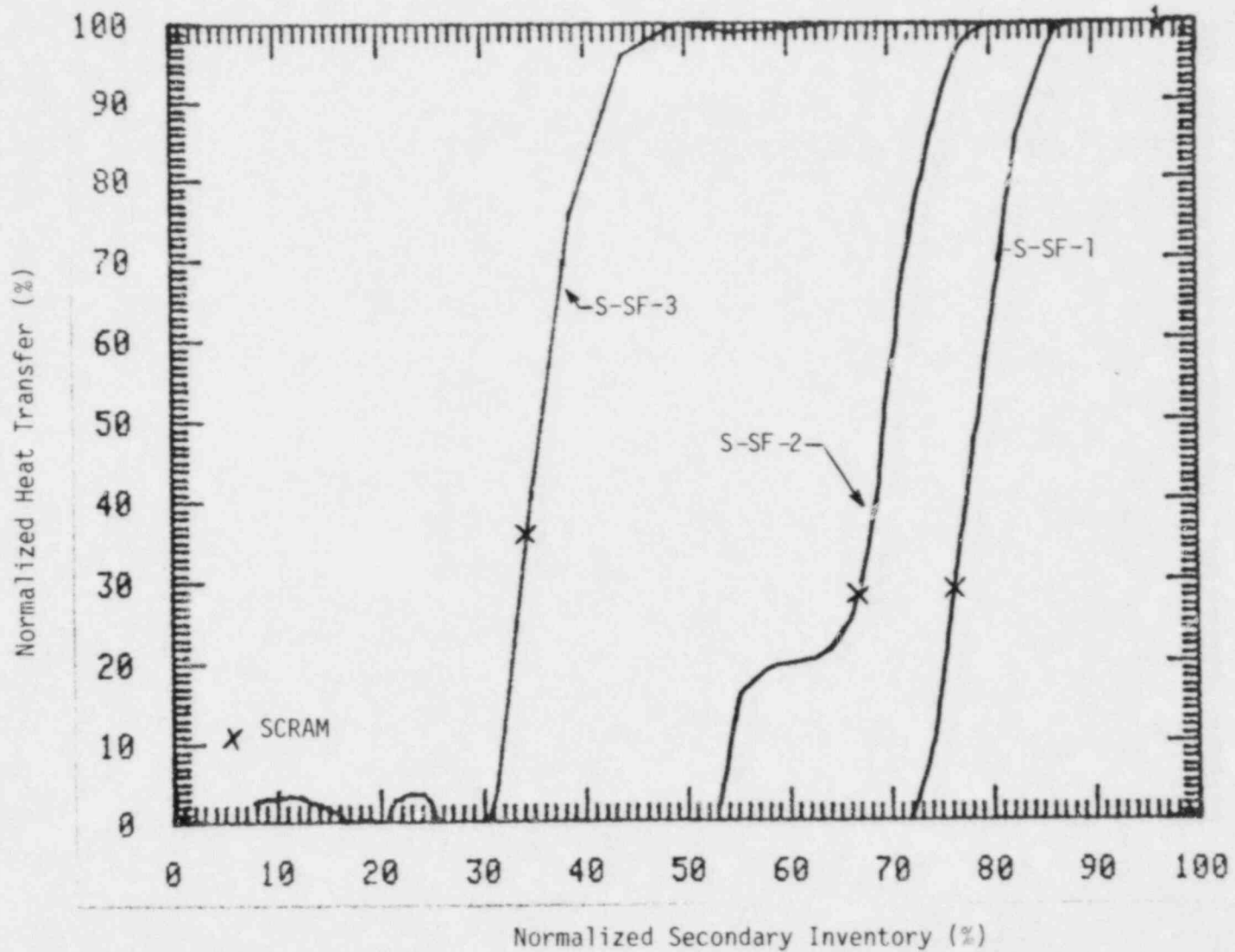


Figure 34. Change in heat transfer rate to broken loop secondary as a function of secondary inventory.

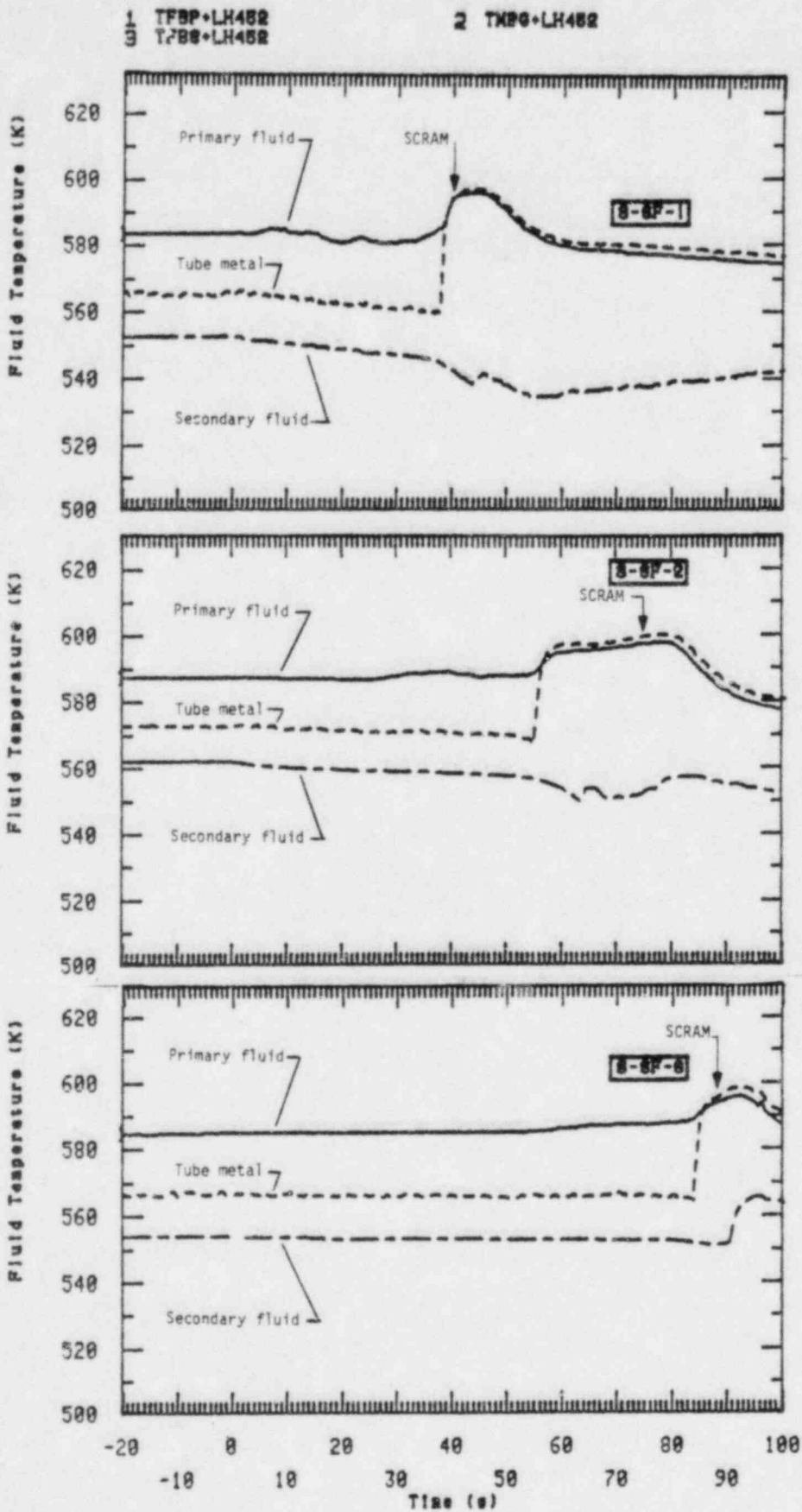


Figure 35. Comparison of primary fluid, tube metal, and secondary fluid temperatures at 452 cm above tube sheet in broken loop steam generator.

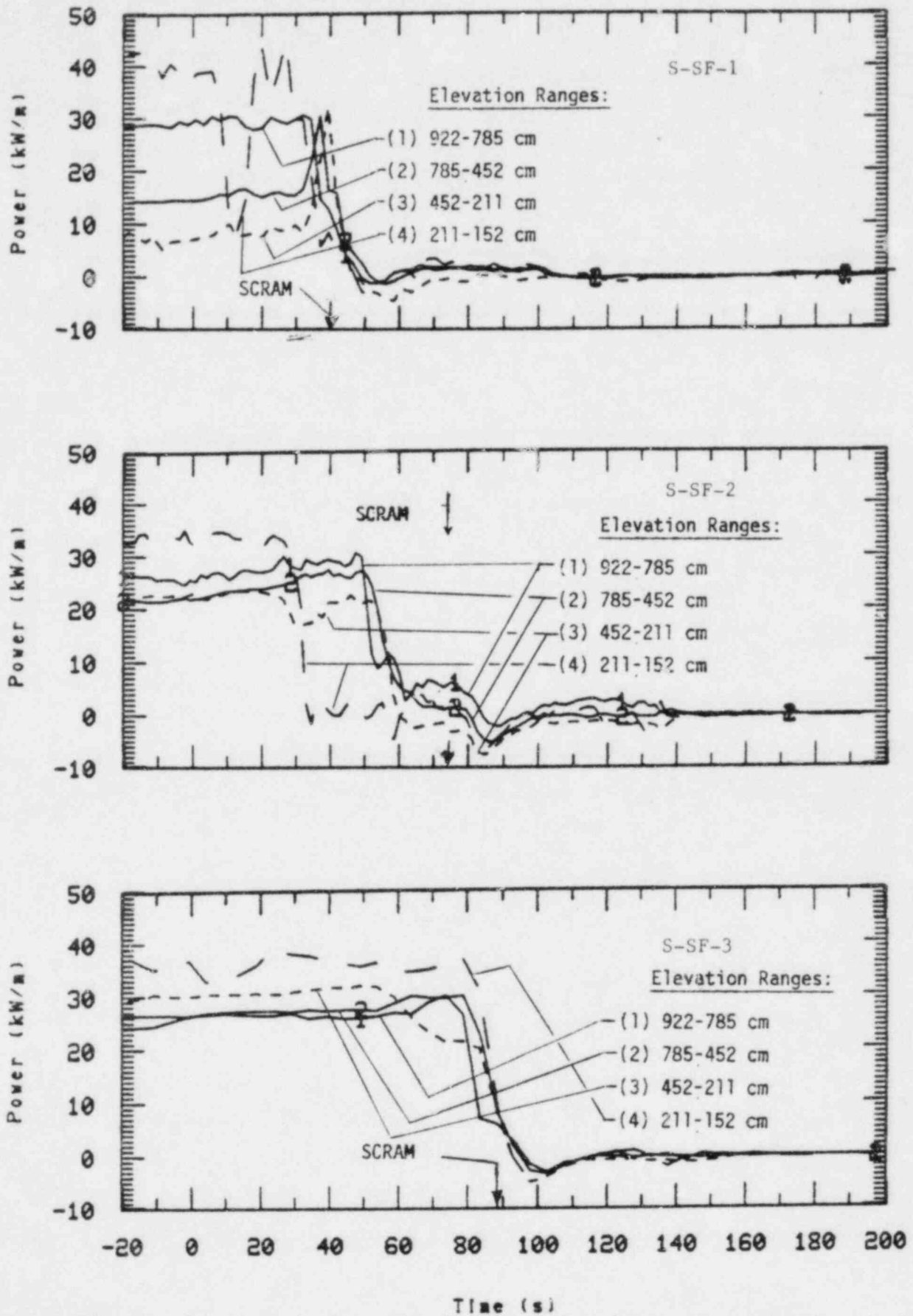


Figure 36. Local heat transfer rates in the broken loop steam generator during Tests S-SF-1, S-SF-2, and S-SF-3. Scram is indicated by arrow.

temperatures, separated by the elevations listed on the figure, and the measured mass flow rate along with the liquid specific heat. These show a very rapid heat transfer degradation almost simultaneously along the entire length of the tubes, with some tendency toward a top-down trend. An exception to this was the early heat transfer degradation that occurred between elevations 152 to 211 cm in Tests S-SF-1, and S-SF-2. As seen in Figure 36, the heat transfer at this elevation fell to near zero well before any other elevations were affected. In Test S-SF-1 (the largest break) it returned to a higher than initial value shortly thereafter, but in Test S-SF-2 it did not recover prior to the overall generator heat transfer degradation. No such behavior was observed in the smallest break experiment (S-SF-3). This behavior is not well understood due to the limited instrumentation available to measure local phenomena in the steam generator. However it is possibly a result of the hydraulics induced by the double-ended blowdown of the generator through both the feedwater and steam line prior to isolation.

The brief period of negative heat transfer (heat transferred to the primary fluid) that is implied in Figure 34 after SCRAM is primarily a consequence of the measurements used to calculate the overall steam generator heat transfer. The fluid thermocouples used are located in the inlet and outlet piping. Consequently, when the primary temperature dropped following SCRAM there was a brief period of time when heat was transferred from the hot primary metal in the plena and piping with little or no heat transfer through the secondary.

Figure 37 shows similar local heat transfer rates in the intact loop generator. Since feedwater flow was terminated the intact loop generator was essentially undergoing a small steam line break transient. As seen by examining the figures, in Test S-SF-1 where the initial inventory was lowest, and Test S-SF-3 where there was an extended blowdown, there was gradual degradation of heat transfer in the upper half of the tubes prior to SCRAM. In Test S-SF-2 the heat transfer remained uniform throughout the generator until SCRAM.

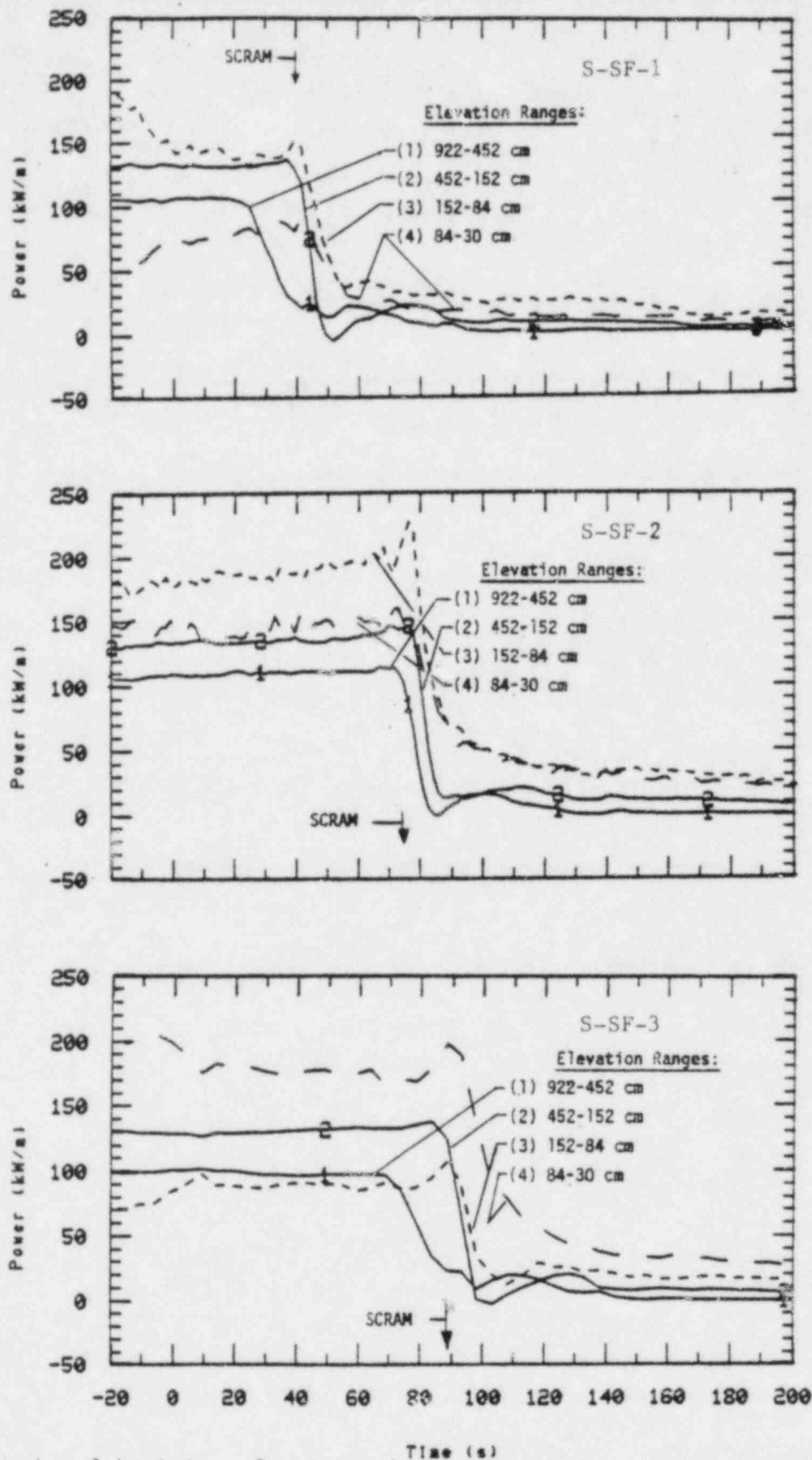


Figure 37. Local heat transfer rates in the intact loop steam generator during Tests S-SF-1, S-SF-2 and S-SF-3.

3.5 Recovery Operations

In Tests S-SF-1 and S-SF-2 system recovery was affected only through the use of primary HPIS injection and secondary side auxiliary feedwater flow. Broken loop auxiliary feedwater flow was terminated at approximately 300 s to simulate operator action upon identifying the affected steam generator. Natural circulation was quickly established in the intact loop after the pumps had coasted down. With the loss of broken loop sink natural circulation virtually ceased in that loop. With the core power set to scaled decay levels, and some reduction in external heater power necessitated by the near stagnation associated with natural circulation, the system was losing more heat than was produced in the core. In conjunction with intact loop auxiliary feedwater injection this caused a continuous depressurization and cooldown of the system. In Test S-SF-2 the shrinkage was such that the primary side of the steam generator tubes in the stagnated broken loop eventually voided.

Once substantial voiding had been detected in the vessel upper head the HPIS flow was boosted to higher flow rates than specified for the head curve used during the blowdowns.^a Once the pressurizer heaters were turned back on the bubble in the vessel upper head began to collapse.

The post-blowdown phase of Test S-SF-3 was used to obtain information on core cooling without secondary heat sinks. Beginning at about 700 s the steam generator secondaries were drained and HPIS injection was terminated. Core power was increased to a constant 60 kW and the system slowly pressurized. Core power was eventually increased to 80 kW (see Figure 38) to help compensate for heat losses. The system was allowed to vent from the pressurizer relief valve at a pressure of 13.1 MPa in order to deplete fluid inventory. (The system pressure is shown in Figure 39 and

a. The curve specified was obtained assuming failure of one train of the HPIS system, which results in about a 22% reduction in flow rate. The flows used for recovery, Figure 9, were reasonably close to scaled injection rates for undegraded conditions.

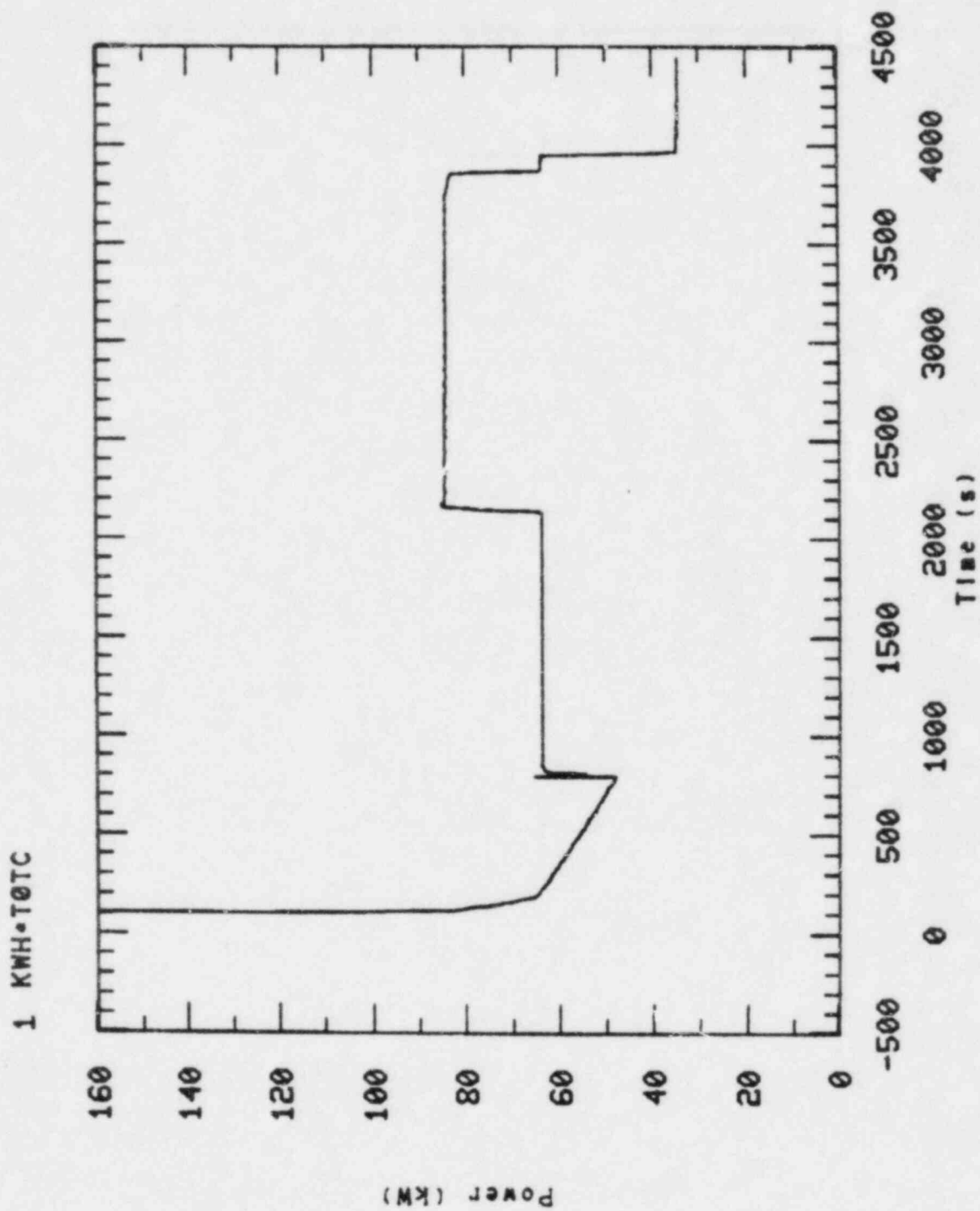


Figure 38. Augmented core power from Test S-SF-3.

1 PV=UP-13

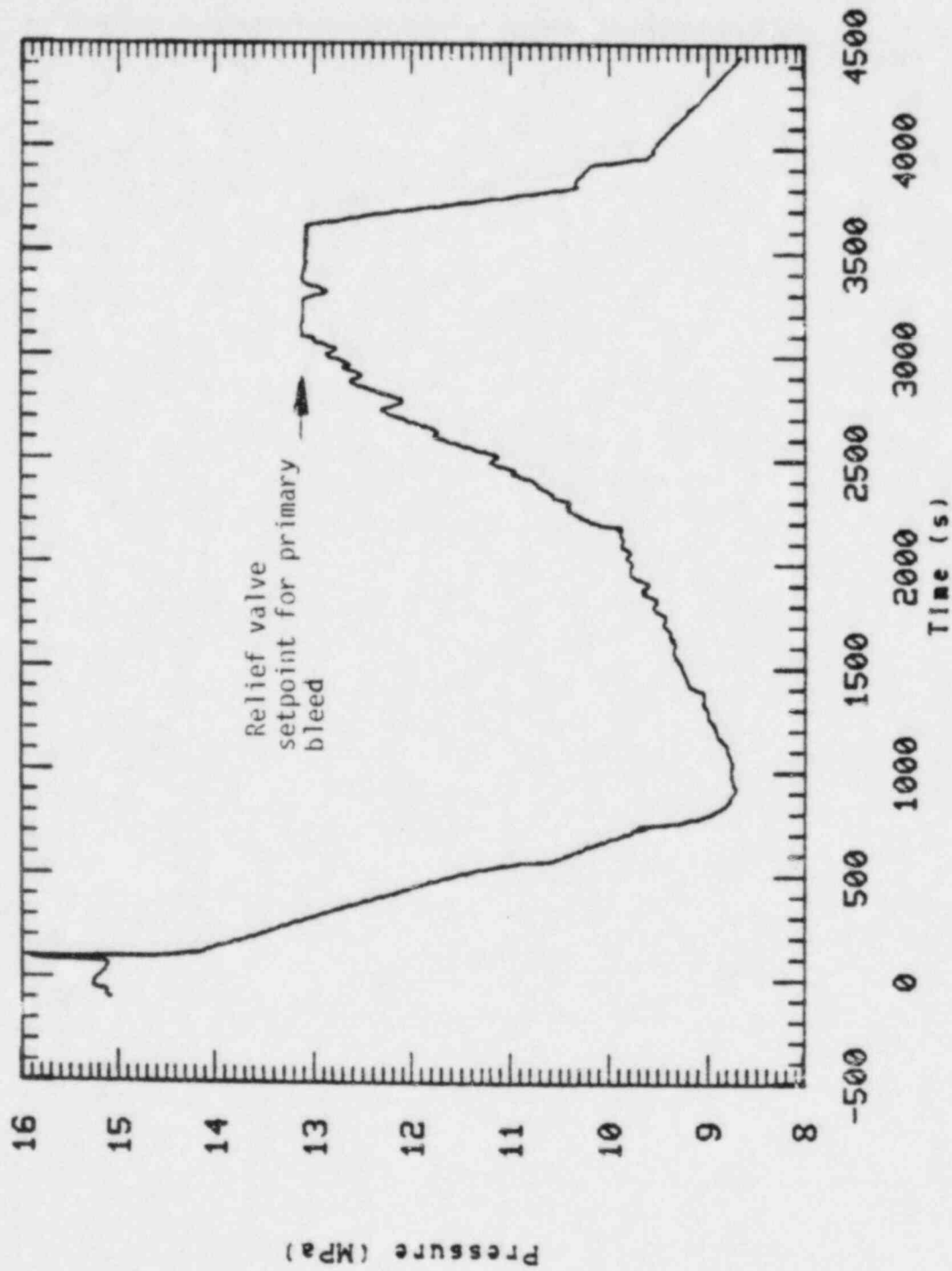


Figure 39. System pressure from Test S-SF-3.

the vessel and downcomer collapsed liquid levels are shown in Figure 40.) The core remained well cooled for over 3000 s after the heat sinks were removed.

Once the first indication of core dryout was obtained, indicating a severely degraded condition, the pressurizer relief valve was latched open to depressurize the system back below the HPIS shutoff head of 12.2 MPa, and accentuate two-phase level swell in the core. Although the downcomer and core collapsed liquid levels indicated a gradual recovery, the rapid depressurization caused a significant redistribution of liquid flashed off from the core. This caused a continued core heat up (see Figure 41). The test was terminated before excessive rod temperatures were obtained. The data will be evaluated as scoping information for future tests aimed at evaluating primary feed and bleed in the absence of secondary heat sinks.

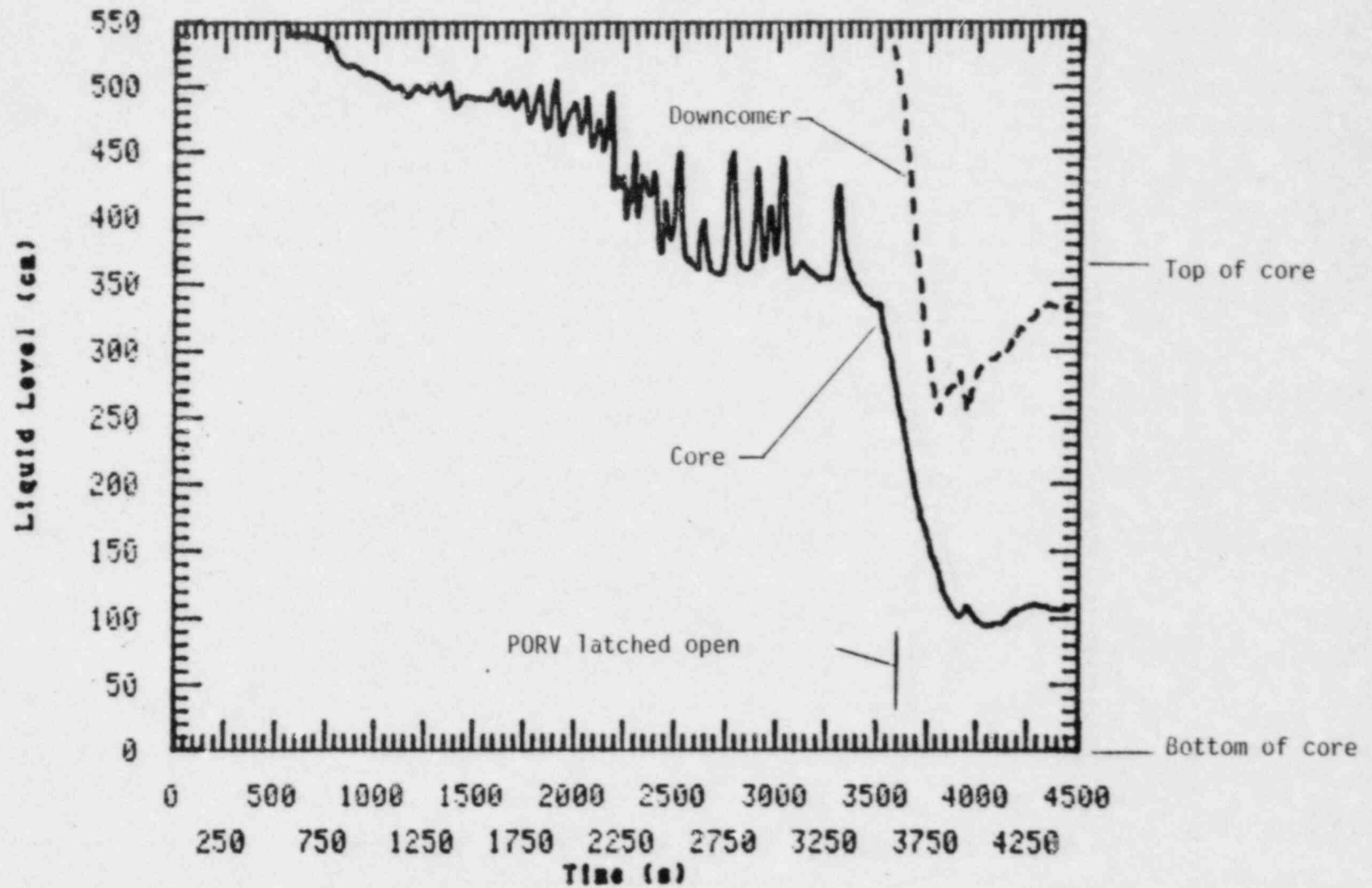


Figure 40. Core and downcomer collapsed liquid levels from Test S-SF-3.

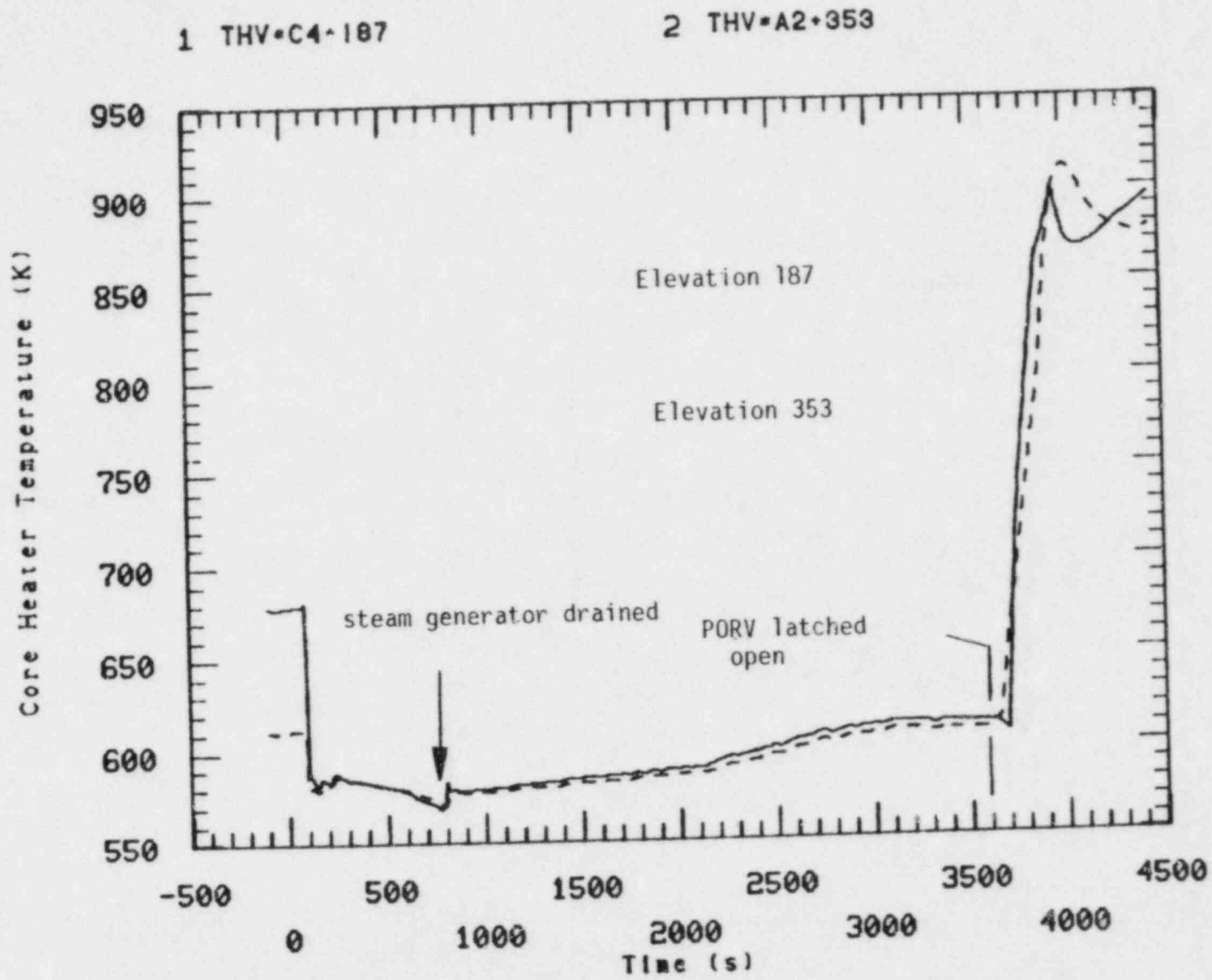


Figure 41. High and mid-core temperatures from Test S-SF-3.

4. CONCLUSIONS

The Semiscale Mod-2A feedwater line break scoping Experiments S-SF-1, S-SF-2, and S-SF-3 accomplished their objectives of; determining the primary-to-secondary heat transfer characteristics as a function of time and secondary inventory for various break sizes, providing a data base for assessment of water reactor safety codes, and providing data for specifying future experiments. The experiments also provided a data base for evaluating accident signatures, with some discrepancies in timing caused by inventory differences, and for evaluating secondary side level measurement behavior during a blowdown.

Results from the tests showed that the primary-to-secondary heat transfer degrades very rapidly (i.e., over approximately a 10-15 percent inventory range), and that the degradation occurs with large amounts of water remaining in the secondary. The inventory at which the onset of degradation occurs was found to be a function of break size, increasing with increasing break size.

The nature of the heat transfer degradation behavior suggests that it is not caused predominantly by loss of secondary inventory per se, but rather by a large decrease in the secondary side heat transfer coefficient resulting from changes in the tube surface hydraulic conditions.

The simple recovery procedures following the blowdowns showed that the system could be brought to a stable condition as long as some minimal secondary heat sink was available to assist natural circulation.

5. REFERENCES

1. D. J. Shimeck, Experiment Operating Specification for Semiscale Mod-2A Steam and Feedwater Line Break Scoping Experiment Series, EGG-SEMI-5830, EG&G Idaho, Inc., March 1982.
2. System Design Description for the Mod-2A Semiscale System, Addendum I, "Mod-2A Phase I Addendum to Mod-3 System Design Description," EG&G Idaho, Inc., December 1980.